Universidad de Concepción
Dirección de Postgrado
Facultad de Ingeniería Agrícola - Programa de Doctorado en Ingeniería Agrícola

“Desarrollo de un sistema de bombeo eólico de acople directo mediante un convertidor de potencia”

(“Development of a direct-coupled wind pumping system driven by a power converter”)

Tesis para optar al grado de Doctor en Ingeniería Agrícola con mención en Recursos Hídricos en la Agricultura

DAVID DOMINGO LARA CASTELLS
CHILLÁN-CHILE
2014

Profesor Guía: Gabriel Merino Coria
Dpto. de Mecanización y Energía, Facultad de Ingeniería Agrícola
Universidad de Concepción

Table of Contents

List of figures

PAPER I

PAPER II

PAPER III

List of Tables

PAPER I

PAPER II

PAPER III

Introduction

Chile's Central Interconnnected Grid (Sistema Interconectado Central - SIC) supplies 99% of the country's electricity [1]. Access to electricity is available, but the inclusion of fossil fuels in the energy mix and the delay in the implementation of hydropower projects have contributed to a steady rise in electricity prices.

As an increase in energy prices has a direct impact on the operating costs of water pumping systems for irrigation, systems based on non-conventional renewable energy (NCRE) have emerged as an alternative to those that operate with traditional energy sources. In fact, irrigation systems based on NCRE are of special interest for the development of small and medium-scale agriculture because energy price is a key factor in production costs for agricultural products.

According to the agricultural census 2006-2007, the total planted or sown area in the coastal communes of the Bio Bio Region ranges from 0.1 to 3.17 hectares per farmer [2]. In fact, the average area per farmer does not exceed 0.5 hectares in 9 of the 14 coastal communes, so that the agricultural activity is carried out mainly by small farmers. These farmers are supported by the government through the National Institute for Agricultural Deveopment (INDAP), by financing the initial cost of equipment used in agricultural activities. As small farmers can not afford pumping systems based on NCRE because of their high cost, these can be eligible for co-financing.

The electrical power required to supply water to the areas mentioned in the previous paragraph ranges between 300 W and 3 kW. It is also important to note that the topography of the coastal area (hillsides) is suitable for applying water gravitationally using pressurized systems with water storage. This means that the coastal dryland presents good conditions for the implementation of water pumping systems based on NCRE.

The use of wind power is restricted to the nearest atmospheric layer to the ground, where the air flow is strongly influenced by local topography and surface roughness characteristics. Wind speed increases significantly in the first few tens of meters above the surface.

The wind regime is mainly controlled by the spatial distribution of the pressure field. The northern and central areas of Chile are under the influence of the South Pacific subtropical anticyclone, located around 30° S in the oceanic sector. This situation favors winds originating from the south in adjacent ocean areas [3].

From Valparaíso Region to Los Lagos Region, typical values of mean speeds are in the range of 2 - 4 m s^{-1}. High values of mean wind speed are recorded in Cristo Redentor (6.9 m s^{-1}), located in the mountains at an altitude of more than 3,000 m and Laja Lake (5.0 m s^{-1}), located at an altitude of 1,375 m altitude. In addition, Puerto Dominguez and Gutamanga in the Chacao channel record mean wind speeds of 6.1 m s^{-1} and 6.7 m s^{-1}, repectively. Both places had measurements for a few years. Throughout this part of the country, locations in the inland valleys along the central depression present low wind

speeds, between 2 and 3 m s^{-1}. This is an example of how local conditions affect the wind speed regime in a given area.

The coastal area of the Bio Bio Region presents features that generate higher mean wind speeds than those recorded in inland valleys, due to the generation of sea breezes caused by temperature differences between the ocean and the mainland. Measurements performed in Cobquecura reported mean speeds between 4 and 5.3 m s^{-1} at an altitude of 10 m above the ground level [3].

Regarding the use of wind power for pumping water for irrigation, standard configurations of wind power systems include the use of batteries for energy storage in order to avoid power fluctuations caused by wind speed variations. This increases the cost of the systems to the point that implementation becomes infeasible. Batteries also require constant maintenance and proper operation to maintain useful life . Moreover, the use of batteries requires the use of power conditioning systems (charge controllers, rectifiers, inverters) both to store energy and supply electrical loads, which reduces the overall efficiency and reliability of the system [4].

A system with battery bank can maintain a relatively constant voltage, allowing the use of electropumps with electric power supply with similar characteristics to the network (220 o 380V/ 50 Hz) through a voltage inverter. This implies that the electropump for the system can be selected in a traditional way, that is by determining the operating point flow rate (Q) - pressure (H), as the intersection point between the Q – H system and pump characteristic curves [5].

There are wind water pumping systems that do not use batteries, such as direct drive systems between the generator and the electropump and those using a power converter to connect the generator and the electropump. In these systems, water is stored in tanks and the electric load is not fixed, as is the battery bank. In addition, control devices are required to manage power flows and optimize captured wind power. As in this case the electropump operates at variable rotational speed, proper operation of pumping systems with direct connection between the turbine or aerogenerator (AG) and the electropump require certain voltage and power relations between these devices.

Direct coupled systems have been developed from the 90s by Vick and Clark, United States Department of Agriculture (USDA). The first step was to develop these systems coupling permanent magnet generators (PMG) with induction motors that operate at similar voltage/frequency rate [6]. Then, protection components were included both at the start of the AG-pump and high frequency zones, that is, against high wind speeds [7]. The theoretical development of these systems has been published by Muljadi *et al*. [8] National Renewable Energy Laboratory (NREL) and Velasco *et al*. [9].

In direct drive systems, the input power presents continuous flunctuations according to wind speed variations. This affects the rotational speed of the electropump, so that it does not remain in a single operationg point as in the case of constant voltage and frequency. Therefore, an electropump for a direct drive wind energy system can not be selected by the method of intersection between H - Q curves described above. Therefore, new selection criteria need to be defined for these variable operating conditions.

The sizing of pump systems with respect to the AG is a key issue for the proper operation of a direct drive pumping system in order to take advantage of a wide range of wind speeds. An undersized pump results in a generator operating at excessive rotational speeds, and causes startup problems on the electropump [9]. These systems find a barrier due to the supply of pumps available on the market. Besides, they lack regulatory mechanisms that allow implementing maximum power point tracking (MPPT) techniques.

Maximum Power Point (MPP) operation depends on the incident wind speed and the rotational speed of the AG. Since wind speed can not be controlled, the rotational speed of the AG can be modified only by adjusting the current generated. In direct drive systems, the AG rotates according to the incident wind speed, which produces a variable rotational speed; when using a PMG, the electrical frequency generated is also variable. The electro pump follows these variations in voltage and frequency, increasing or decreasing its own rotational speed, and acting as an unregulated electrical load.

Recent research focuses on pumping systems using direct drive power converters. The system studied by [10], is especially remarkable and consists of the implementation of a MPPT control system for a converter of a 3.76 kW pumping system. Even though the strategy used shows an effective tracking of the maximum wind efficiency point, it is important to note that mechanical speeds for both the generator and the pump need to be measured, which requires a larger number of sensors.

The cost of batteries, as well as operation and maintenance costs are eliminated when using direct coupled wind-electric power pumping systems with a power converter. In addition, these systems present greater flexibility when selecting the electro pump because they are

provided with control power components. MPPT algorithms can also be implemented, which allows optimizing the captured wind resource.

One way to achieve the MPP operation is the regulation of the current generated. From the viewpoint of the generator, the current acts as a braking torque, which opposes the torque exerted by the wind through the turbine. Therefore, the rotational speed increases or decreases according to the balance of these torques. If the pump operating point is modified by manipulating the electrical frequency, the required current also changes, and consequently the braking torque also changes.

To make these changes in the pump operating point, it is necessary to incorporate a power converter. Firstly, this allows decoupling the frequency between the AG-Motor, so that the frequency to the motor is controlled independently from the PMG frequency. Secondly, it enables the implementation of MPPT control strategies, using the motor as a regulated electric load, which allows for varying degrees of load to the generator, controlling the rotational speed and the electric power produced.

Hypothesis

It is hypothesized that wind-electric pumping systems could be operated based on controllers that allow maximum power point tracking and direct coupling between the aerogenerator and the electropump, avoiding the use of batteries.

Objetives

OVERALL OBJETIVE

To develop and evaluate a direct coupled wind-electric pumping system driven by a static power converter that allows maximum power point tracking and does not requiere the use of batteries.

SPECIFIC OBJETIVES

- To quantify the efficiency of a small-power wind pumping system with battery bank in each stage of power conversion.
- To develop and evaluate a static power converter that allows direct coupling between the aerogenerator and electropump, tracking the maximum power point.
- To quantify the effect of wind speed and electro pump operation at variable rotational speed on the pumping capacity of the system.

Thesis structure

The body of this thesis consists of three manuscripts submitted for publication.

The first article analyzes a wind-electric pumping system with small power battery bank. Power measurements are made for each component involved in the process of energy conversion in order to determine the overall efficiency of the system. Based on these measurements, efficiency of each component is determined and, with this, the overall efficiency. The power curve of the aerogenerator of the system and its power factor are also determined. This article states the need to develop new configurations due to the large amount of energy dissipated in the components of the pumping system.

The second article discusses the advantages of direct drive wind-electric pumping systems with power converter over pumping systems with battery banks. A power converter was implemented to connect directly a single-phase electro pump and the aerogenerator. Furthermore, two control algorithms for the power converter were developed and compared. These control algorithms allow operating the pump at variable rotational speed, aiming at pumping water at a wide range of wind power available.

Finally, the third article analyzes the hydraulic behavior of centrifugal and peripheral pumps operating at variable rotational speed. Direct drive wind-electric wind systems operate under fluctuations in wind speed that produce variations in the generated electric power supplied to the pump. This results in the operation of the pump under fluctuating power supply and variable rotational speed. The use of a power converter can regulate

rotational speed by control algorithms. The effect of two algorithms is analyzed regarding pump rotational speed and flows rated.

Paper I

Efficiency Assessment of a Wind Pumping System

by

David D. Lara, Gabriel G. Merino, Boris J. Pavez, Juan A. Tapia

Efficiency Assessment of a Wind Pumping System

David Lara, Gabriel Merino, Boris Pavez, Juan Tapia

ABSTRACT

The combined efficiency of the components determines overall system performance in electric wind pumping systems. We evaluated a system composed of a 3 kW wind generator feeding a battery bank of 48 V / 880 Ah by means of a non-controlled 6-pulse rectifier. Connected to this battery bank was a 1.5 kW inverter that generated 220 V at 50 Hz, which powers a 1.1 kW single-phase electric pump. At the University of Concepcion, Chile, energy losses in each electrical component was determined using a data collection system configured to measure electrical variables in real time. The electrical power generated by the wind generator for different wind speeds averaged 38% lower than the power curve provided by the manufacturer. Electromechanical tests performed in a lab showed the operation efficiency of the electric generator of the wind turbine averaged 80%. This information, along with the electrical power output, and the wind velocity measured during field operation allowed us to determine the rotor's power coefficient C_p, which had a maximum value of 35%. For the stored energy components measured data indicated that the rectifier, the battery bank, and the inverter operated with average efficiencies of 95%, 78% and 86% respectively. The combined component efficiencies showed a maximum of 17% of the wind energy would be available for water pumping. Since a large amount of

wind energy was dissipated during the energy conversion process, new configurations should be analyzed that could avoid such losses in wind pumping systems.

INTRODUCTION

In Chile, there are 555,276 rural families, 37,644 of whom do not have access to electricity, 95.2% of rural families receive power from the grid, 4.2% have their own or a community diesel generator and 0.5% have photovoltaic panels. However, in those places with no grid, a considerable percentage of electrical energy is provided by internal combustion generators, as an example in the XIth and XIIth regions of Chile 13% and 45%, respectively, of the electricity is generated by diesel generators.

The National Energy Commission's (CNE) Rural Electrification Program (PER) aims to draft technical feasibility studies on electrification projects based on renewable energies. In 2001, a pilot project was implemented on Isla Tac (Xth Region) using a hybrid wind-diesel system with two 7.5 kW wind generators providing electricity to 79 families. The PER has enforced small wind generators (WG) be incorporated into distributed generator systems or as part of hybrid, wind-solar or wind-diesel systems.

Wind power in rural areas is also widely used to pump water by means of mechanical systems and electric-wind systems. The formers show higher efficiency at low wind velocities whereas electric-wind systems show better efficiency at high wind velocities. The electro-wind pumping systems present greater annual efficiency related to the water pumped, about 10% to 15%, compared to 5% or 6% for a mechanical system of the same rotor diameter [1]. On the other side, the electrical systems have the added advantage that

the turbine can be located on a site with a better wind profile and not necessarily on the site where the water is pumped [2].

Wind electrical systems for water pumping are expensive because, generally speaking, they require 5 components to convert the wind energy into electrical energy (WG, rectifier, charge controller, batteries and inverter). A less expensive system can be obtained by connecting the electric pump to the generator with a controlled converter, which provides safe operating conditions for both the WG and the electric pump [3]. This method reduces the number of components and allows the power storage in the battery bank to be replaced by a water storage tank. A storage tank is most feasible where the morphology of the land allows locating the tank at a convenient height that permits distribution of the water gravitationally.

Low-power wind turbines generally operate in isolated systems and frequently the energy is stored in battery banks. The behaviour of low-power aerogenerators has been reported by Muljadi et al. [4] and Bowen et al. [5]. They developed equivalent circuits based on electrical theory. Power control systems have been developed by Tan and Islam [6] and Ermis et al. [7], which allow the wind generator to operate at maximum transfer of power conditions. In general, the studies conducted on these systems analyze each component in particular without taking into consideration the system operation and efficiency as a whole. Therefore, when a power output forecast is made, the percentage of losses produced in each component as well as the losses in the entire system is unknown, making it difficult to draft reliable energy predictions for a certain period of time.

Furthermore, knowing the efficiency of each electric component plays a key role in the suitable dimensioning of the required wind generator.

According to the above, the aim of this work was to determine the overall efficiency and the efficiency of each electric component of an electro-wind pumping system. To this end, an electro-wind system was evaluated using a 3 kW WG feeding a battery bank of 48 V and 880 Ah by means of a non-controlled 6-pulse rectifier. Connected to the battery bank was a 1.5 kW inverter that generated 220 V at 50 Hz, which fed a 1.1 kW single-phase electric pump. The power flows were measured by a data collection system implemented to measure electrical variables in real time. The efficiency of the WG was determined by a load test performed in the laboratory. The measurements and tests were performed at the University of Concepcion, Chile.

Efficiency in the electro-wind systems

In the electro-wind pumping system studied, batteries are used to store energy and different electrical components are used to convert the wind energy for storage and/or to pump water. The generator, the charge controller, the batteries and the inverter make the process of converting energy available in the wind to electrical energy that can be used for the electric charge. This process sees different types of energy losses, which limit the system's efficiency.

The energy conversion process begins with the power available in the wind P_V [8]:

$$P_{\mathrm{V}} = \frac{1}{2}\rho \mathrm{A}\mathrm{V}^3 \qquad (1)$$

Where ρ is the air density, *A* is the turbine swept area and *V* is the wind speed. The wind power is converted into mechanical power (P_{mec}) by the turbine blades, according to the equation:

$$P_{\text{mec}} = C_p \cdot P_V \quad (2)$$

Where, C_p is the power coefficient of the turbine, which is a function of the wind speed *V* and the blade rotation speed ω. The maximum theoretical value of C_p is 0.59 according to the Betz limit. In practice, the values of C_p fluctuate between 0.25 and 0.40 [9], since aerodynamic losses are produced in the blade due to attrition, drag torque and mechanical design [10].

The mechanical power is converted into 3-phase alternating current (AC) electrical power by the generator. In the generator, different losses are produced; losses in the stator winding caused by the copper resistance, losses in the iron due to parasitic currents and hysteresis and losses due to the gap between stator and rotor. Therefore, the generated electrical power is the mechanical power in the axis multiplied by the generator efficiency η_{gen}:

$$P_{\text{elec}} = \eta_{\text{gen}} \cdot P_{mec} \quad (3)$$

The 3-phase AC electrical power (P_{elec}) leaving the generator is in turn converted into direct current (DC) electrical power (P_{DC}) by the rectifier for storage in the battery bank. In

this process, power in the charge controller is dissipated due to commutations of semiconductors in the rectifier [11]:

$$P_{\mathrm{DC}} = \eta_{\mathrm{rec}} \cdot P_{elec} \tag{4}$$

Where, η_{rect} is the rectifier's efficiency.

It is not possible to characterize the battery bank's efficiency through the power. In this case, the accumulated energy in Amperes–hours or Watt–hours are used instead; hence, the battery efficiency (η_{bat}) is defined as the amount of energy extracted from the battery (E_{out}) divided by the amount of energy necessary to restore it to its initial state of charge (E_{in}) [12]:

$$\eta_{bat} = \frac{E_{out}}{E_{in}} \tag{5}$$

Finally, the energy stored in the battery bank (E_{bat}) is transformed into power in AC by the inverter, thus:

$$P_{inv} = \eta_{inv} \cdot P_{DC} \tag{6}$$

Where η_{inv} is the inverter efficiency, P_{inv} is the inverter output and P_{DC} is the power input in the inverter.

The system's overall electric efficiency (η) is given by the product of the efficiency for each one of its components:

$$\eta = \mathrm{C_P} \cdot \eta_{\mathrm{gen}} \cdot \eta_{\mathrm{rect}} \cdot \eta_{\mathrm{bat}} \cdot \eta_{\mathrm{inv}} \tag{7}$$

EXPERIMENTAL SETUP

The electro-wind pumping system analyzed in this study was installed at University of Concepcion, Chillan Campus, Chile, latitude 36º32' south, longitude 72º06' west. The WG studied was a 3 kW rated WG of two blades, 4.6 m in diameter, operating at variable speed. The turbine was located 25 m above the ground on a tubing tower. A 16-pole synchronous alternator on the WG generates alternating current with variable voltage and frequency. The three phase WG nominal voltage is 48 V, as well as the battery bank voltage and inverter voltage.

The power generated by the WG is connected to a charge controller located 30 m from the tower via underground three-phase wires of 8 AWG gage.

The AC power delivered by the WG is rectified in order to deliver DC current an voltage required by the batteries. This is done by the controller of charge, included by the WG manufacturer in the wind generation group, which contains a non-controlled 6-pulse rectifier, with its output directly connected to the battery bank. The charge controller unit is also connected to a power dissipater, which dissipates the surplus energy in the form of heat when the battery bank is completely charged. The DC power is stored in a nominal 48 V/ 880 Ah battery bank, consisting of 32 deep cycle batteries of 6 V and 220 Ah. The DC power from the batteries is transformed into AC by a DR 1548E Trace 1.5 kW single-phase inverter (Xantrex Technology Inc., Vancouver, Canada) , which powers 1.1 kW electric pump.

The system was monitored from December 2006 to February 2007. The electrical variables were measured by a data acquisition system (DAS) to determine the power flows between the individual components of the system.

Data acquisition systems (DAS)

In order to monitor the electro-wind pumping system, two DAS were implemented. The first measured the wind speed and the second measured and recorded the electrical variables of each component.

On a meteorological tower located 30 m from the wind generator, a NRG #40 anemometer (NRG Systems, Hinesburg, Vermont) was installed which had an accuracy of 0.1 ms^{-1}, for a wind speed the range of 5 to 25 ms^{-1}. The anemometer was located at the same height as the WG. A BasicStamp (Parallax Inc., Rocklin, California) microcontroller sampled the wind speed at a rate of 5 Hz and recorded the averaged every 10 seconds in a computer. Accuracy of wind velocity measurements is affected by many factors such as; the DAS characteristics, surface roughness, and installation conditions. The uncertainties of the wind velocities measurements was assessed based on the Standard IEC 61400-12 [14]. The prevailing winds were from the South, for measurements reported here. Even when the distance between anemometer and de WG is grater than four times the rotor diameter (18.4 m), the nearest obstacle that could affect the wind profile around the meteorological tower and turbine is located 400 m away. Furthermore, the surrounding terrain is flat with a roughness coefficient (z_0) equals 8 mm, corresponding to a short grass.

The DAS for measuring electrical variables was configured to measure the power flows between the system components. This DAS was synchronized with the wind speed DAS. System currents were measured with HAS-50S (LEM, Genova, Switzerland) Hall Effect sensors with an accuracy of 1% at 25°C, and system voltages were measured by LV-25P (LEM, Genova, Switzerland) voltage transducers with an accuracy of 0.9% at 25°C. The sample rate for this sensors was 1 ms in order to obtain the frequency and rms values. The locations of the voltage and current transducers are shown in Figure 1. The uncertainties associated to voltage and current transducers were calculated based on the full scale value for each one of the measured variables. The maximum uncertainty for current was 0.531 A at a full scale of 50 A. On the other side for voltage, the maximum uncertainty was 1.282 V at a full scale of 80 V.

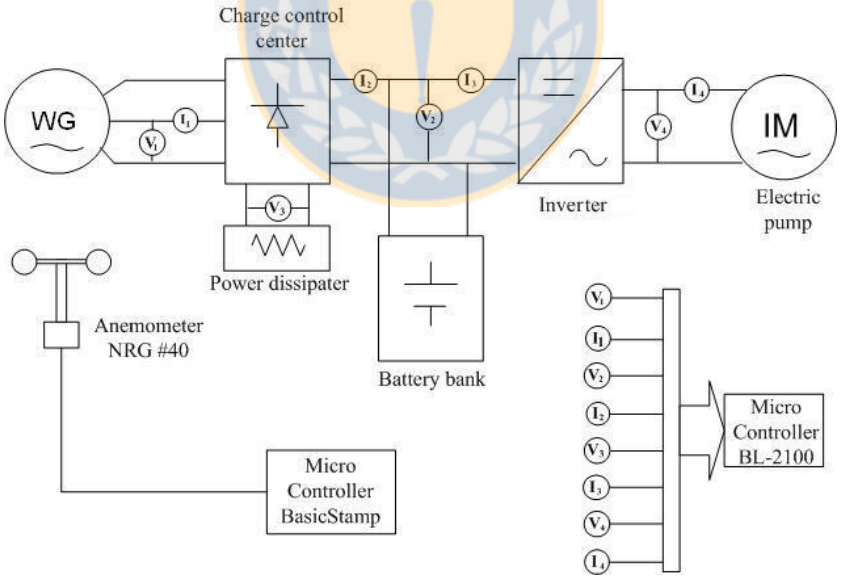

Figure 1. Locations of current and voltage transducers in the electro-wind pumping system.

Table 1. Electrical variable sensed by each transducer.

Electric variable	**Symbol**
Generator AC voltage	V_1
Generator AC current	I_1
Pump AC current	I_4
Batteries DC voltage	V_2
Pump AC voltage	V_4
Batteries DC current	I_2
Inverter DC current	I_3
Power Dissipater DC voltage	V_3

Table 1 shows the electrical variable sensed by each transducer. The sensor outputs were connected to a Rabbit BL2100 (Rabbit, Davis, California) microcontroller card, which recorded the voltage and current values every ten seconds synchronously with the wind speed DAS.

RESULTS

Empirical determination of the WG power curve and the system efficiency

The electro-wind pumping system was monitored from December 2006 to February 2007. The data collected by the DAS were stored until a representative amount of data had

been obtained for each wind speed range according to the Chilean Official Standard, NCh 2946-2 [14], which is based on the Standard IEC 6400-12.

An operating strategy for the system was defined in order to determine the generator's electrical power curve versus wind speed, the efficiency of each component and the overall efficiency for the electro-wind pumping system. To this end, the system was divided into two operational parts, the first part included the WG and the charge controller; this part was monitored with the inverter disconnected, so that all the generated electrical power could be stored in the battery bank until it was fully charged. This allowed the power curve of the WG and the fluctuation in the charge controller's efficiency to be determined. The charging period of the battery bank fluctuated between 5 and 9 days, depending on the wind speed distribution. The second part of the experiment concentrated on the operation of the battery bank, coupled to the inverter and the electric pump. This part was monitored with the WG disconnected; thus, all the power entering to the inverter came from the battery bank, thus, when the input and output power in the inverter was measured its efficiency could be determined. The duration of the discharge period varied slightly depending on the charge status reached by the battery bank, the time of discharge fluctuated between 24 and 25 hours. The batteries were discharged at 80%. During the 3-month monitoring period, it was possible to make four charge-discharge cycles for the electro-wind system.

The total energy stored in the battery bank was obtained by measuring the voltage and current coming out from the rectifier to the battery bank. Similarly, when the power output from the battery bank was integrated, the total energy discharged was obtained. By dividing these two results, the efficiency of the battery bank was obtained according to equation 5.

Wind generator power curve versus wind speed

The WG power curve was obtained by applying the Method of Bins, which consists of classifying the data measured in bins of wind speed 0.5 ms^{-1} wide and centered at integer multiples of 0.5 ms^{-1}. Each wind speed bin had to include a minimum of 1,800 data points of wind speed and power generated. The average wind speed V_i and power generated P_i for each interval were obtained according to the following equations:

$$V_i = \frac{1}{N_i} \sum_{j=1}^{N_i} V_{i,j} \quad (8)$$

$$P_i = \frac{1}{N_i} \sum_{j=1}^{N_i} P_{i,j} \quad (9)$$

Where:

$V_{i,j}$: Wind speed measurement *j*, at interval *i*.

$P_{i,j}$: Electrical power measurement *j*, at interval *i*.

N_i : Number of data at interval *i*.

Figure 2a shows distribution of power generated us a function of wind velocity. At wind velocities lower than 5 ms^{-1}, the standard deviation from the average could make the power generated grater than the power as provided by the manufacture, this is due to the fact that the mechanical response of the anemometer is faster than the wind turbine response. In contrast, at medium and high wind velocities, the standard deviation from the average decreases, and the power generated is lower than the values provided by the manufacture.

Figure 2b shows the WG mean power curve versus wind speed according to the wind speed and power data measured in the field. For wind speeds lower than 3 ms^{-1}, the WG has a rotational speed close to 200 rpm, but the system did not generate any power, since the voltage generated was insufficient to polarise the rectifier's diodes. During the measurement period, the wind speed did not exceed 16 ms^{-1}. Figure 2b also shows a comparison between the power curve provided by the manufacturer and the one obtained in the field. The mean power curve measured is obviously lower than the one indicated by the manufacturer, which could directly affect the estimation of the energy during a certain period.

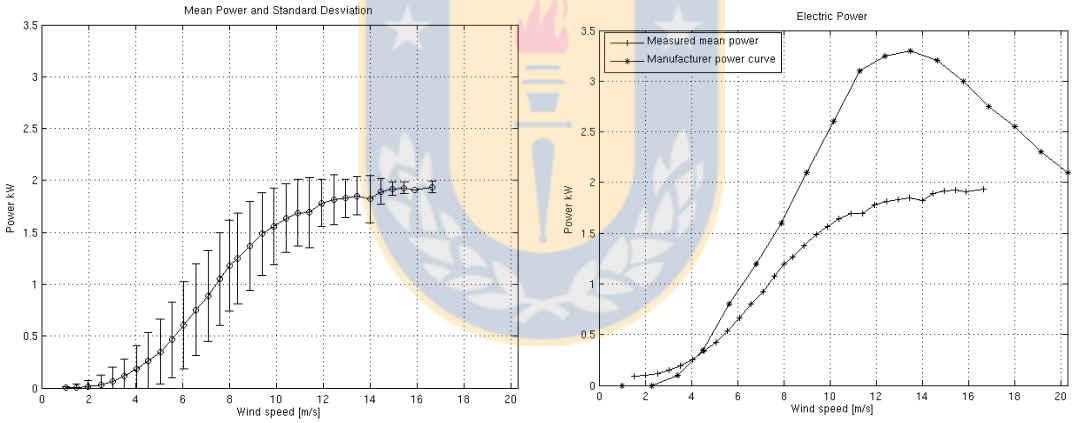

(a) (b)

Figure 2. Measured power curve: (a) average power curve and standard deviation (b) Comparison between the manufacturer's WG power curve and the power curve obtained in the field.

The uncertainty in the above curves is associated to power, voltage and current transducers and also to the DAS. The maximum power uncertainty, ±1%, value correspond to medium wind velocities where the wind turbine operates during more time [14].

Voltage and current curve vs. rotation speed

Figure 3 illustrates the line-by-line voltage and the phase current measured in the WG terminals as a function of the rotation speed in the range of 0 to 800 rpm. The data set corresponds to 48 hours of measurement, obtained on January 12 and 13 of 2007. The voltage variations between 0 and 200 rpm have a linear behaviour. Between 200 and 300 rpm, a curvature is produced in the output voltage which reaches a constant value of 60 V. The voltage and current uncertainties were ±1.65% and ±1.1% respectively.

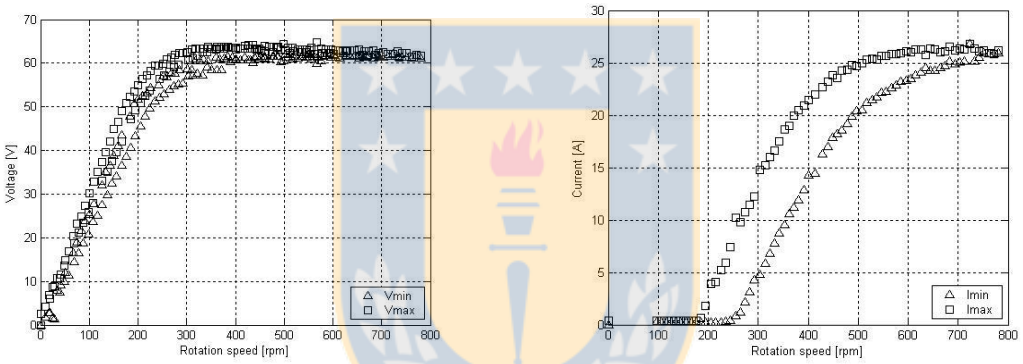

(a) **(b)**

Figure 3. WG voltage and current as a function of rotation speed: (a) AC voltage, (b) AC current.

For low rotation speeds, when the voltage generated is insufficient to polarize the diodes, the voltage has a linear behavior following the relation of the FEM to the rotation speed (fig.3a). Around 200 rpm, the DC voltage generated is greater than the battery voltage, the diodes are polarized and current begins to circulate. As the rotation speed increases, the frequency increases and the impedance value becomes greater, limiting the current to a value below 27 A (fig. 3b). It can also be seen that for the same rotation speed, there is a range of current values, which is due to voltage variations in the battery bank. The higher

the voltage of the battery bank, the smaller the voltage difference between the WG voltage and the battery bank voltage and therefore, a lower current is delivered to the batteries. These variations in the current significantly affect the average WG power curve, causing fluctuations that can reach 480 W. Bowen et al. reported similar results for this operating condition; for a given wind speed, there are differences in the generated power, and this affects the average WG power curve [5].

In order to take into account air density effect on the wind power generated, air temperature and atmospheric pressure were measured during field testing process. The wind turbine is located at 137 m above sea level. From de collected data, it was concluded that air density fluctuated between 1.160 and 1.225 kg m^{-3}, according to the equation:

$$\rho = \frac{P}{RT} \tag{10}$$

Where P is the atmospheric pressure in Pa, R is the gas universal constant 287.05 J $kg^{-1}K^{-1}$ and T is the absolute temperature in K. Thus, in the worse scenario, power output variations due air density are 5% related to standard air density at sea level.

Efficiency of the permanent magnet synchronous generator (PMSG)

In order to evaluate the losses and efficiency of the PMSG, tests were conducted in the Machine Laboratory of the Electrical Engineering Department at the University of Concepcion.

Figure 4 shows the diagram of the electromechanical driver used as a driving force for the PMSG under test conditions. This driver comprised a direct current motor (DCM). The

field coil was fed independently using a variable DC source, fixing its current at 0.9 A. The armature coil was fed through a three-phase variac and a 6-pulse rectifier, which made it possible to vary the motor's rotation speed by controlling the armature voltage and to operate the WG at different speeds. The characteristics of the continuous current motor are presented in table 2.

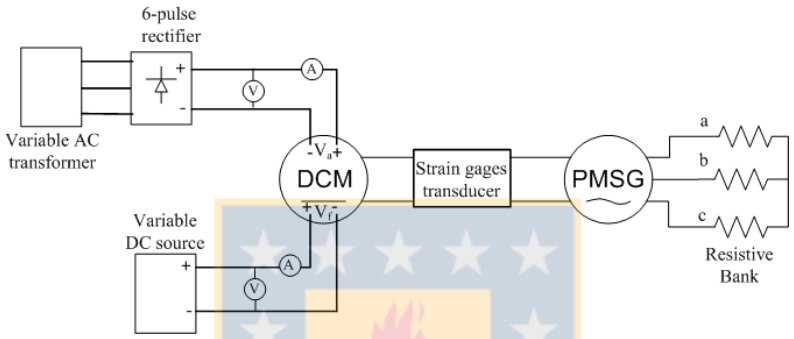

Figure 4. Diagram of the PMSG's electrical driver.

Table 2. Characteristics of the continuous current motor.

Power [HP]	5
Speed [rpm]	850/2600
Armature current [A]	19
Armature voltage [V]	240
Field current [A]	0.9/0.27
Field voltage [V]	240

A strain-gage transducer type MA-06-250BF-350 (MTM, Raleigh, North Carolina) with an accuracy of 1.5% was installed on the axis of the PMSG (fig. 4), which delivers a

variable amplitude DC voltage proportional to the distortion produced in the axis to which it is attached. This enables the PMSG's power input to be calculated as the product of the torque and the rotation speed. The torque per volt sensed in the axis was obtained from the following equation:

$$T_{FS} = \frac{(V_{FS} \cdot \pi \cdot E \cdot 4 \cdot (D_o^4 - D_i^4)}{V_{EXC} \cdot GF \cdot N \cdot 16{,}000 \cdot (1 + v) \cdot G_{XMT} \cdot D_o} \quad (11)$$

In which:

D_i : Internal diameter of the axis (mm).

D_o : External diameter of the axis (mm).

E : Elasticity module, $E = 206.8 \times 10^3$ (Nmm^2)

GF : Gage factor.

G_{XMT} : Telemetry transmitter gain.

N : Number of active gages, $N = 4$.

T_{FS} : Maximum torque for a 10 V output (NmV^{-1}).

V_{EXC} : Excitation voltage from the jumper (5 V).

V_{FS} : Maximum voltage delivered by the system (10 V).

v : Poisson constant (0.3 for iron).

During the above tests, resistance banks were used as electrical load. Output power from the PMSG terminals was measured by an oscilloscope model OS-5020 (EZ Digital Co. Ltd, Seoul, Korea) using the wave forms of the voltage signal and current generated. Dividing

the output power from the generator by the mechanical power in the turbine axis, the PMSG efficiency was obtained at different rotation speeds. The rotation speed was varied between 200 to 400 rpm (Fig. 5). When the rotation speed increased, both the input to the generator and the output increased, so that the generator efficiency could be determined at different speeds.

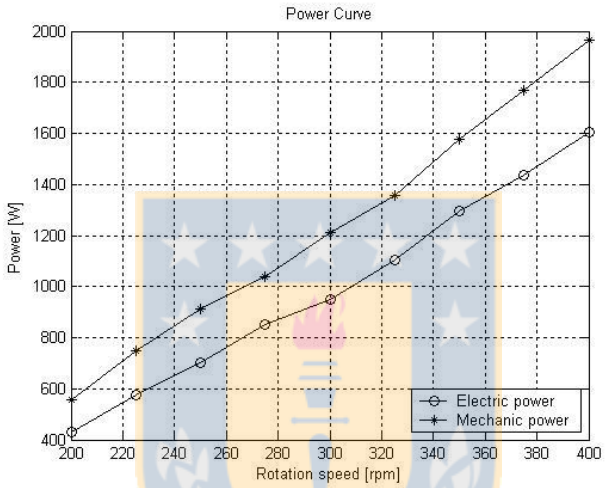

Figure 5. Input and output power in the PMSG.

The generator measured efficiency is shown in Figure 6. For the speed range from 200 to 260 rpm, the losses by armature current are small, with the mechanical losses and those from magnetization being the most prevalent. The average efficiency achieved by the PMSG was 80% with an uncertainty of ±3%.

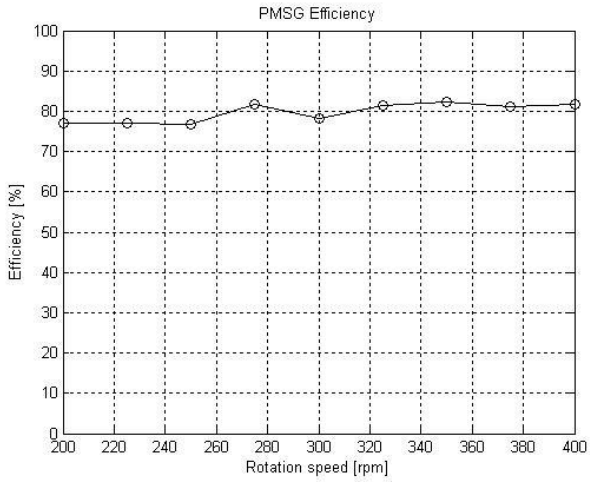

Figure 6. Efficiency curve measured for the PMSG.

Estimating the power coefficient C_p

From the electrical power, P_{elec} , generated by the WG and the efficiency of the PMSG, η_{gen} , measured in the laboratory, an estimation can be made of the mechanical power P_{mec} in the axis of the WG under field operation. Dividing the mechanical power by the wind power P_V , the turbine efficiency or power coefficient C_p is obtained as:

$$C_p = \frac{P_{mec}}{P_V} \tag{12}$$

On the other hand, when the wind speed measured is related to the rotational speed of the WG, the tip-speed ratio (TSR) λ is obtained as:

$$\lambda = \frac{r \cdot \omega}{V} \tag{13}$$

Where r is the radius of the turbine, ω is the rotation velocity in rads^{-1} and V is the wind speed in ms^{-1}.The rotational speed was calculated from the relationship between electrical and rotational frequency, according to the equation:

$$n = \frac{120 \quad f}{P} \tag{14}$$

Where f is the frequency of the voltage generated, P is the number of magnetic poles and n is the rotational speed.

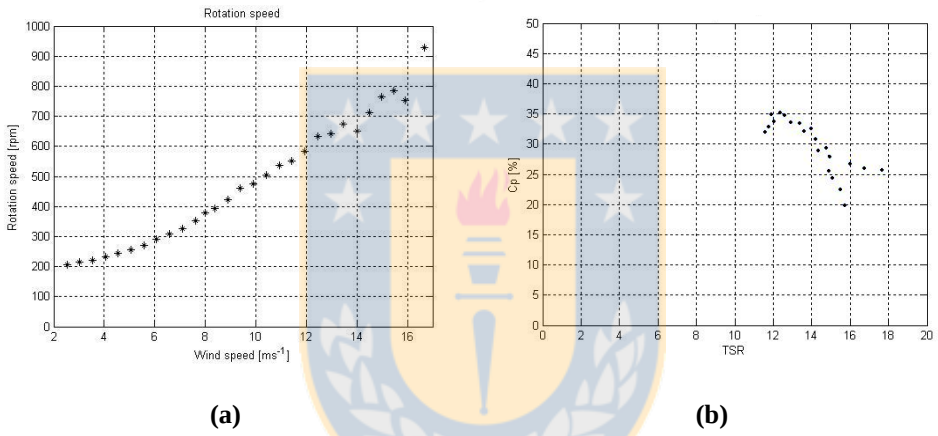

Figure 7. (a) Rotation speed vs. wind speed and (b) Power coefficient vs. tip-speed ratio (TSR) .

Figure 7a shows the relationship between rotational speed and wind speed. The rotational speed ranged between 200 to 900 rpm, for wind speeds from 2 to 17 ms^{-1}. At low wind speeds, 2 to 3 ms^{-1}, the WG is spinning due to the WG inertia. In addition, high wind speeds, 16 to19 ms^{-1}, produced discontinuities in the curve due to the WG aerodynamic protection (furled).

Figure 7b shows the variations in the power coefficient C_p of the wind turbine under operation as a function of the TSR and wind speed. When the wind turbine starts to

generate power, which happens around 200 rpm, depending on the battery bank voltage, there is a wind speed of 3 ms^{-1}, which means a TSR in operation equal to 16. In addition, the rated power of the WG is obtained at a wind speed of about 10 ms^{-1}, as in figure 7b; the average rotation speed at this wind speed is 500 rpm, which implies a TSR of 12, at which the peak power coefficient is also obtained. From this point, the power coefficient starts to decrease again. Figure 7b indicates that the maximum mechanical power that can be generated by the turbine rotor is about 35% of the power available in the wind. To obtain the above C_p curves, a generator efficiency of 80% was accounted for.

Efficiency of the 6-pulse rectifier (Graetz Bridge)

Figure 8 shows the data regarding the efficiency of the rectifier on December 6 of year 2006. This data set comprises the second charge cycle made to the system. The efficiency was obtained by dividing the output and input power in the rectifier measured simultaneously.

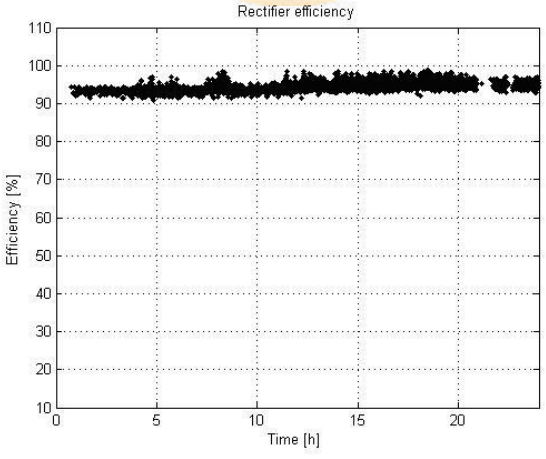

Figure 8. Rectifier efficiency as a function of time.

The rectifier efficiency fluctuates between 90.9% and 98.5%. These variations depend on the rotation speed of the WG, which governs the amplitude of the voltage and its frequency. The rectifier efficiency tends to increase with the increases in wind speed. The average efficiency achieved was 94.4% with a maximum uncertainty of ±2.5%.

The inverter efficiency

When the inverter is started up, it starts to feed the electric pump, extracting power from the batteries. The power data for this test were collected during complete battery bank discharge cycles. The ratio between the inverter output and the power delivered by the batteries is the efficiency at which the inverter operates.

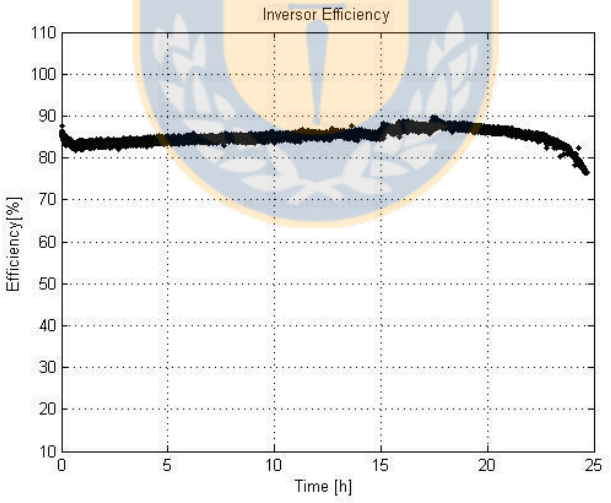

Figure 9. Inverter efficiency as a function of time.

Figure 9 shows that the inverter efficiency fluctuates between 76.6% and 89.6%. During the first hours of discharge, the output practically stays constant and decreases together

with the voltage that the batteries can deliver; the average inverter efficiency was 85%, with a maximum uncertainty of ±2.5%. The efficiency increases as the voltage from the battery bank reaches its nominal voltage of 48 V. In general, inverter instruction manuals indicate the peak efficiency for a certain degree of charge. In this case, the peak efficiency indicated is 95% [13].

Efficiency of the battery bank

The efficiency of the battery bank was assessed using the ratio between the energy extracted from the battery bank (E_{out}) and the energy required to get the battery into its initial state of charge (E_{in}), as stated in equation 5. Charge-discharge cycles performed from December 2006 to February 2007 were performed to this end. Values of the energy input and energy output are presented in Table 3 as well as the efficiencies obtained.

Table 3. Efficiency of the battery bank.

	11-Dec-06	**21-Dec-06**	**08-Jan-07**	**19-Jan-07**
Ein [kWh]	42.1	41.4	43.9	43.4
Eout [kWh]	33.2	32.5	33.8	33.5
Efficiency [%]	78.9	78.5	77.0	77.2

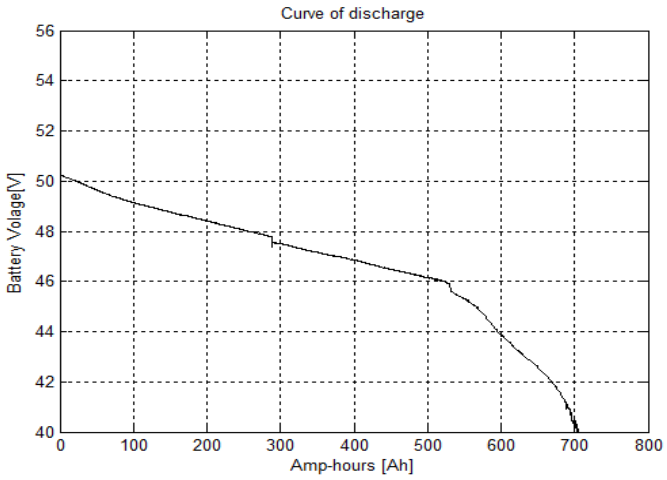

Figure 10. Curve of battery bank discharge.

Figure 10 shows the curve of the battery bank discharge for 8 January of 2007. The energy extracted from the bank reached 700 Ah, reaching a minimum battery voltage of 40.4 V. The average efficiency for the battery bank was 77.9 % ±2.5%.

Analysis of the charge-discharge cycle

In order to determine the efficiency of the system, the energy transferred during different charge-discharge cycles was determined. During the charge cycle, the inverter stayed off so as not to affect the charge status of the batteries. For the discharge cycle, the WG remained disconnected so that the electrical pump would consume the power stored in the battery bank during the previous charge cycle. Then the amount of energy at each of the stages of the energy conversion process was determined. The results are presented in Table 4.

Table 4. Summary of the energy transferred during the charge-discharge cycles.

Energy [kWh]	11-Dec-06	21-Dec-06	08-Jan-07	19-Jan-07
Electric energy generated	44.8	43.7	45.8	46.3
Energy input to Batteries	42.1	41.4	43.9	43.4
Energy input to Inverter	33.2	32.5	33.8	33.5
Energy input to Pump	28.6	28.5	29.0	28.7

Table 5. Efficiency of the system components.

Efficiency [%]	11-Dec-06	21-Dec-06	08-Jan-07	19-Jan-07
Rectifier efficiency	93.1	94.7	95.9	95.9
Batteries efficiency	78.9	78.5	77.0	77.2
Inverter efficiency	86.1	87.8	85.8	85.7
Electric system efficiency	63.3	65.4	63.4	63.5

The efficiency of each electric component is presented in table 5. By multiplying the efficiency of each one of the components, the overall electric system efficiency it is obtained and is presented in the bottom row of table 5. In average 63.9% of the electrical energy generated by the turbine is left available for pumping water, with approximately 36% dissipating through the energy conversion processes.

CONCLUSIONS

An electro-wind pumping system was tested and evaluated. Analyzing the different stages of the energy conversion process, it was possible to develop an efficiency analysis of the system. This analysis included measuring the WG power curve, the efficiency of each component and the system's overall efficiency.

From the wind speed and the power generated by the WG data collected during operation in the field with the DAS, it was possible to generate the wind turbine power curve. This evaluation indicated that the electrical power measured for different wind speeds is significantly less than the WG power curve provided by the manufacturer: 30%, 36% and 49% less at wind speeds of 6, 10 and 13 m s^{-1} respectively. These values can be affected by atmospheric conditions and installation conditions by the user.

Through electromechanical tests performed in a lab, it was determined that the operation efficiency of the PMSG is of about 80%. This information and the electrical power output and wind velocity measured under actual field operation conditions allowed to determination of the rotor's power coefficient C_p. The maximum value reached by this coefficient was 35% which corresponds to the maximum percentage of the power available in the wind that could be converted to mechanical power on the WG axes.

On the other side, a data acquisition was installed in the field to assess the efficiency of each electric system component under field operation conditions. The results indicate that the rectifier works with an efficiency of about 95% in average. The battery bank operates

with an efficiency of 78% in average and the inverter operates with an average efficiency of 86%.

According to the above, as a maximum, the turbine blades could convert 35% of the kinetic energy available in the wind into rotational energy. From this energy 51% could be lost by the electrical components of the system; rectifier, batteries, and inverter. This means that, as a maximum, only 17% of the energy available in the wind could be available for water pumping. Since a considerable amount of energy is lost during the energy conversion process, new configurations should be developed and analyzed that could avoid such losses in wind pumping systems.

ACKNOWLEDGEMENTS

The authors wish to acknowledge the financial support of the Fondo de Desarrollo para la Ciencia y la Tecnología FONDECYT (project N° 1040506) Chile and the University of Concepcion.

REFERENCES

[1] Vick, B.D. and R.N. Clark. 2000. Testing of a 2-kilowatt wind-electric system for water pumping. In Proceedings of Windpower 2000 Annual Conference. 9-19.

[2] Miranda M., Lyra R., Silva S., An alternative isolated wind electric pumping system using induction machines, IEEE transactions on Energy Conversion, 1999, 14(4): 1611-1616.

[3] Velasco M., Probst O., Acevedo S., Theory of wind-electric water pumping, Renewable energy, 2003, 29(6): 874-893.

[4] Muljadi E, Buakasuewucz JT, Analysis of the dynamics of a wind-turbine water-pumping system, In Power Engineering Society Summer Meeting, 2000:2506-2519.

[5] Bowen A.J., Zakay N., Ives R.L., The field performance of a remote 10kW wind turbine, Renewable energy 2002, 28(1): 13-33.

[6] Tan K., Islam Syed, Optimum control strategies in energy conversion of PMSG wind turbine system without mechanical sensors, IEEE transaction on energy conversion 2004, 19(2): 394-399.

[7] Ermis M., Ertan H.B., Akpinar E., Ülgüt, Autonomous wind energy conversion system with a simple controller for maximum-power transfer, IEE proceedings 1992, 139(5): 421-428.

[8] Bansal R.C., Bhatti, T.S., Kothari D.P., On some of the design aspects of wind energy conversion systems, Energy Conversion, 2002; 43(16), 2175-2187.

[9] Ozgener O., A small wind turbine system (SWTS) application and its performance analysis, Energy Conversion and Management 2006, 47(11-12), 1326-1337.

[10] De Broe A.M., Drouilhet S., Gevorgian V., A peak power tracker for small wind turbines in battery charging applications, IEEE transaction on Energy conversion 1999, 14(4): 1630-1635.

[11] Hart W. Daniel, Electronica de potencia 2nd ed, Madrid: Prentice Hall; 2001.

[12] Armenta C, Prediction of battery behaviour in SAPV applications, Renewable energy 2003; 28(11), 1671-1684.

[13] Xantrex Technologiy Inc. *Installation and operator's manual for the Xantrex DR Series Inverter/Charger*. 2000., Arlington, USA. Avalaible at: http://www.xantrex.com.

[14] Chilean Official Standard NCh 2946, Wind turbine generator systems. Part 12: Power performance measurements techniques. CNE-PNUD-GEF. Santiago. Chile. 2005.

Paper II

Power converter with maximum power point tracking MPPT for small wind-electric pumping systems

by

David Lara, Gabriel Merino, Lautaro Salazar

Power converter with maximum power point tracking MPPT for small wind-electric pumping systems.

David Lara, Gabriel Merino, Lautaro Salazar

ABSTRACT

Direct-drive wind electric pumping systems with power converters have several advantages over pumping systems that use battery banks. The former require less maintenance and present a lower cost and increased reliability. However, as wind-electric pumping systems do not have a voltage stabilizing stage, the converter needs to handle variations of wind power production and operate the pump at variable rotational speeds.

In this work, an AC-DC-AC direct-drive power converter was implemented for a wind electric pumping system consisting of a permanent magnet generator (PMG) of 1.3 kW and a peripheral single phase pump of 0.74 kW. In addition, the inverter linear V/f control scheme and the maximum power point tracking (MPPT) algorithm with variable V/f were developed. MPPT algorithm seeks to extract water in a wide range of power input using the maximum amount of wind power available. Experimental trials at different pump pressures were conducted. When working with a MPPT tracking system with variable V/f, a power value of 1.3 kW was obtained at a speed of 350 rpm and a maximum operating hydraulic head of 50 m. At lower operating heads pressures (between 10 and 40 m), variable V/f control increases the power generated by the GIP compared to the linear V/f control. This increase ranged between 4% and 23% depending on the operating pressure, with an average of 13%, getting close to the

maximum electrical power curve of the PMG. The pump was driven at variable frequency reaching a minimum speed of 0.5 times the rated speed. Efficiency of the power converter ranges between 70% and 95% with a power factor between 0.4 and 0.85, depending on the operating pressure.

Keywords. *Wind electric pumping, MPPT, Wind energy.*

INTRODUCTION

Most wind-electric pumping systems implemented until now in Chile are designed to store energy in a battery bank and supply loads at 220 V at a frequency of 50 Hz. These systems are generally operated by non-qualified personnel, resulting in poor maintenance, improper storage and defective operation of the battery bank, which are essential to maintain the battery bank's shelf [1].

Wind-electric pumping systems can be found in different powers levels. Systems that consume less than 400 W are adequate to supply water for home use and irrigation of vegetable gardens and greenhouses. These generally use membrane pumps or submersible pumps operated with direct current (DC) motors. Systems with power outputs ranging from 400 to 1,500 W are capable of delivering enough water to irrigate surfaces up to three hectares through the use of technified irrigation [2]. These systems use either centrifugal or peripheral pumps operated with alternating current (AC) motors and are fed from battery banks connected through a charge controller or an inverter [3].

By removing the battery bank from the system and using a water storage tank, all the problems associated with storage, maintenance and operation of electricity in batteries are avoided. As Chile presents an extensive costal line with low mountains along the coast, storage tanks and gravity-fed irrigation systems can be used, eliminating the use of a battery bank. However, when operating under these conditions, the variable power flow generated goes directly from the source to the pump unit and lacks the stabilizing stage provided by the battery bank. Therefore, it is necessary to adapt the operation of the pump to these temporary fluctuations.

The literature describes four types of wind-electric pumping systems without energy storage in battery banks. One of these systems consists of the direct coupling between the wind turbine equipped with a permanent magnet generator (PMG) and the pump, which in turn consists of an induction motor (IM) and a centrifugal pump [4], [5]. This system is easy to implement, but operating procedures and safety measures should be taken into account at both low and high wind speeds. In addition, there must be a relationship between the power of the generator and the motor in order to take advantage of a wide range of wind speeds. If the motor is undersized, there will be an excessive angular velocity in the generator or the system will definitely not run.

Another type of system consists of a self-excited induction generators (SEIG) feeding a pump as the one described in the previous system. In this case, these systems use a capacitor bank to produce excitation voltage and static reactive compensation systems (SVC) to adjust variations in power flow [6], [7].

The third type of wind-electric water pumping systems corresponds to direct current systems that use a PMG, an AC-DC converter and brushless-type DC pumps. There are two manufacturers of these systems: Grundfos and Bergey.

The fourth type corresponds to systems with static power converters. These systems have been developed for hybrid hydro-wind plants, which store water in large tanks using wind-powered pumping and generate electricity in peak hours [8]. They are suitable for the accumulation of wind power as hydroelectric power in islands and non-interconnected systems. They can provide more than 600 kW with several wind generation units as well as pumping units.

The use of wind-electric pumping systems that require small power and use power converter has been scarcely reported [9]. In this power range, water pumping systems powered by photovoltaic energy are frequent [10]–[12]. In these systems, the power converter consists of a chopper and an inverter capable of controlling the power flow absorbed by the pump and operates the photovoltaic arrangement at maximum power point.

Converters can control the power flow to the pump. They also allow the implementation of maximum power point tracking systems (MPPT) and less complex control algorithms for low power pumping systems. Different schemes and MPPT algorithms for wind energy systems have been published. Most of these are appropriate for storage battery systems using DC/DC converters [13]–[15].

The aim of this work is to study a wind-electric pumping system with a static frequency converter of small power. This system seeks to take advantage of the use of low power PMG, as well as the pumping characteristics of pumps that use single-phase induction motors.

As the system can be an alternative for wind-electric pumping systems with battery banks, this work also studies the use of a converter capable of controlling power fluctuations from the PMG. The inverter control scheme and MPPT algorithm are also studied. Both of them seek to extract water in a wide range of power by taking advantage of the maximum power available.

Characteristics of a wind-electric pumping system with a power converter

The electric-wind pumping system studied consists of a wind turbine, a permanent magnets generator (PMG), a static power converter and a single-phase induction motor that powers a peripheral type pump, as shown in Figure 1. The wind generator captures and transforms wind power into three-phase electricity of variable amplitude and variable frequency according to changes in wind speed. Subsequently, a rectifier converts AC to DC power, and then to single-phase AC power by controlling frequency using an inverter. Finally, the inverter operates the pump at a variable rotational speed pushing the flow of water from the suction point to the discharge point.

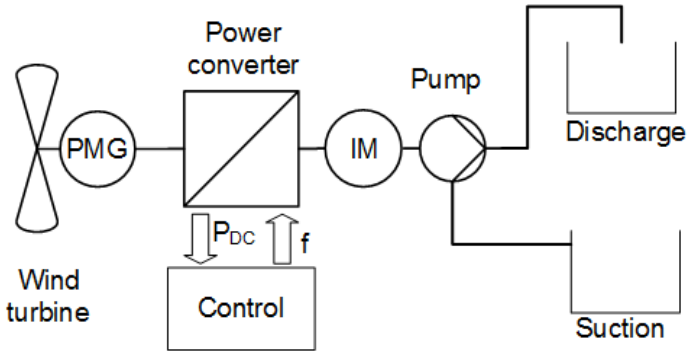

Figure 1. Wind- electric pumping system with a power converter.

Wind turbine

The mechanical power captured by a wind turbine depends on air density ρ, swept area of the turbine A and wind speed V, as shown in Equation 1:

$$P_m = \frac{1}{2}\rho A V^3 C_p \quad (1)$$

C_p is the power coefficient of the turbine, the ratio between the captured power and the available power in the wind. The C_p value is not constant; it depends on the wind speed and rotational speed of the turbine ω related through blade tip speed λ.

$$\lambda = \frac{\omega R}{V} \quad 2)$$

The characteristics of the typical captured power are shown in Figure 2. It can be observed that there is a maximum power value for each wind speed value. For higher power, it is desirable to work as close to the power curve as possible[16], changing the rotational speed of the turbine [17]. At wind speeds above the nominal value of the turbine, captured power should be limited by means of power dissipation and even by stopping the turbine in order to prevent damage to the system.

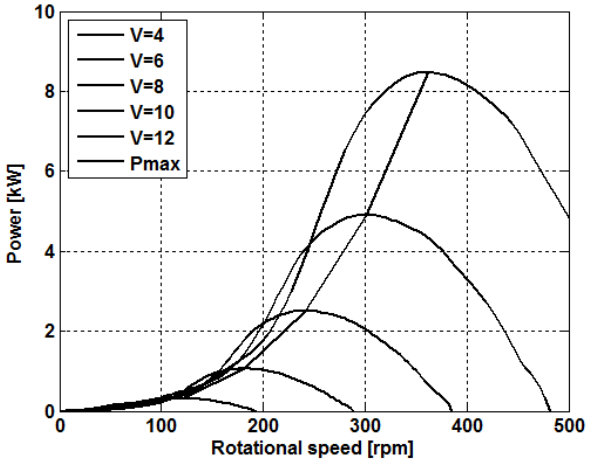

Figure 2. Graph of captured power versus rotational speed at different wind speeds.

Permanent magnet generator (PMG)

The use of a PMG in small power wind-powered systems offers important advantages in construction and operation. As a PMG has a single winding, it weighs less and its power density increases. It has a large number of poles, avoiding the use of speed multipliers and allowing operation at reduced rotation speeds [18].

PMGs have constant magnetic field excitation. Therefore, the induced voltage is directly related to rotational speed and presents variable amplitude and frequency. Table 1 [19] shows the main characteristics of the PMG used in this study. Figure 3 shows the output power and the open circuit voltage curve shown of the PMG. This generator supplies a power output of 1,300 W at a rotational speed of 380 rpm, with an induced voltage of 326 V, providing the power required to supply the system load.

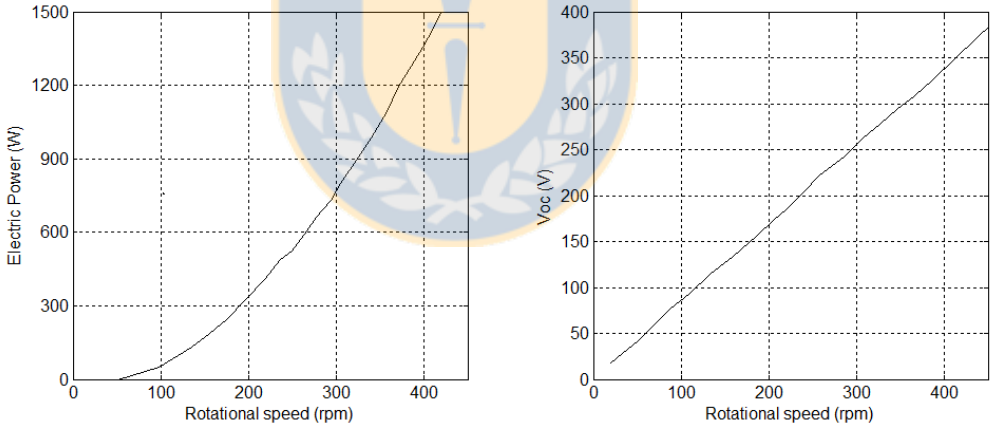

Figure 3. Characteristics of the permanent magnet generator PMG-1800 (a) Power curve (b) Voltage curve at open circuit.

Table 1. Characteristics of the permanent magnet generator PGM-1800.

Output power (W)	**1800**
Nominal rotational speed (rpm)	480
Rectified nominal current (A)	6
Phase Resistence (Ohm)	5
Configuration	Three-phase, star connection
Weight (kg)	19.5
Start-up torque (Nm)	<0.9
Rotor inertia (kgm^2)	0.013

Hydraulic pump

The hydraulic pump is formed by a single-phase induction motor to which a peripheral pump is attached. Induction motors are widely used in water pumping activities because they are robust and inexpensive machines. In fact, they require little maintenance and are easily replaceable in case of failure [20].

A single-phase IM is a device designed to operate at a fixed rotational speed. Variable frequency devices have not been applied to single-phase IMs for different reasons, such as start-up problems, low operating speed close to the centrifugal switch, complexity vs cost, and controllability [21]. In general, methods such as fractional coils, voltage amplitude control and triac semiconductors are used to cut the applied voltage waveform [22].

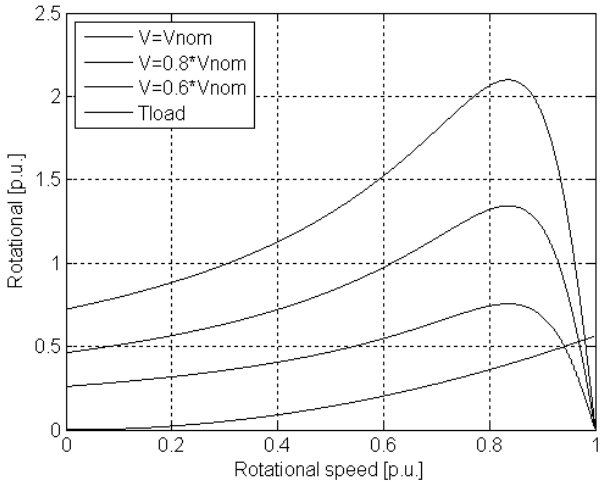

Figure 4. Torque characteristics of a single-phase IM through voltage amplitude control.

Voltage control methods decrease the electrical torque produced by the motor, as shown in Figure 4. This results in a reduced mechanical rotational speed of the motor and an increased slip, which in turn produces power loss in the motor.

Adding a driven variable frequency can offer potential energy savings, especially when loads being driven present a torque which is a function of rotational speed, such as fans and pumps [23]. When controlling the V/f ratio of the motor, the mechanical rotational speed varies, while retaining most of the torque characteristics (Figure 5). Therefore, the slip is small and less power loss is produced in the motor.

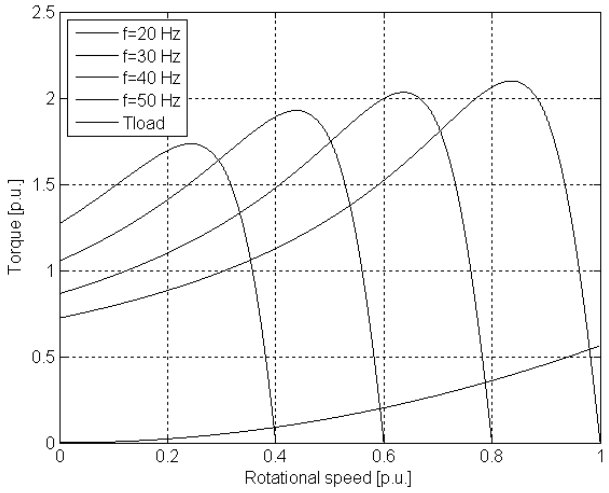

Figure 5. Torque characteristics of a single-phase IM at a constant V/f ratio.

In this study, the IM will be driven at a variable speed with a frequency control system through power converters. Characteristics of the single-phase IM used are shown in Table 2.

Table 2. Characteristics of the single-phase induction motor (IM).

Output power (W)	**750**
Nominal rotational speed (rpm)	2,900
Nominal current (A)	5.6
Nominal voltage (V)	230
Number of poles	2
Capacitor	Permanent type

AC-DC-AC Converter.

The converter implemented for the wind-electric pumping system has the function of controlling the flow of variable power, so as to operate the pump according to the control law. It comprises three stages: a 6-pulse uncontrolled Graetz bridge rectifier of 600 V and 15 A maximum, a link capacitor of 2,590 uF to filter voltage fluctuations from the rectifier and the current from the inverter that follows a $\sin^2(\omega t)$ [24], and a single-phase H-bridge inverter (Figure 6).

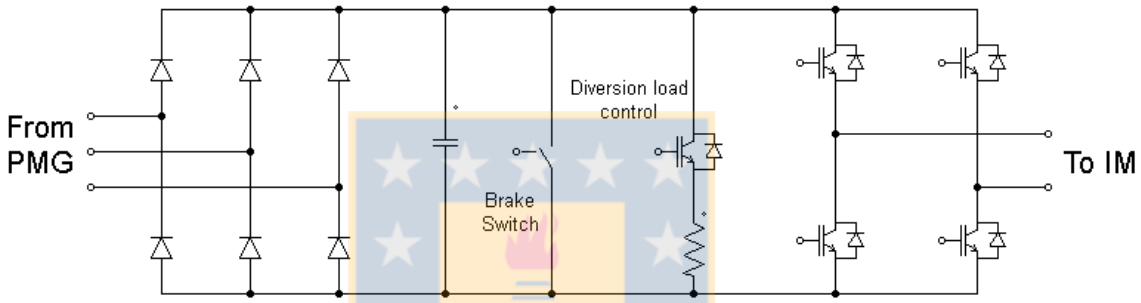

Figure 6. Diagram of the converter for the wind-electric pumping sytem.

The inverter consists of four IGBT in a H-bridge configuration. A medium frequency was used in order to reduce the number of switches and reduce power losses in the transistors [25]. The inverter could power pumps up to 1 kW. The voltage level was selected based on the maximum voltage corresponding to DC link voltage 311 V. Therefore, the IGBTs should withstand at least this voltage. The IGBT selected was the IRG4PC40UD, which is manufactured by International Rectifier.

Characteristics of the control stage of the power converter

The control stage of the power converter consists of a microcontroller, a signal conditioning board and a trigger circuit for the IGBTs of the converter. An algorithm is incorporated into

the microcontroller program, using adequate voltage modulation techniques for motor operation as well as maximum power point tracking routines.

The microcontroller is able to store the required commands to generate the necessary waveforms to control the frequency of inverter [26]. The microcontroller generates trigger signals for the IGBTs based on the control voltage signals and current received. The control algorithm was created and implemented in a microcontroller, including a PWM technique to generate voltage waveform to power the pump. The Arduino Mega 2560 was used since this microcontroller presents a proper frequency range to generate switching signals and PWM ports. Generation of alternating voltage with variable frequency and amplitude is done using PWM ports, which provide trigger pulses with different activation times for each IGBT.

To generate trigger pulses of different width, it is necessary to use two timers in the microcontroller and a lookup table with the values of a half-cycle of the sine function stored in the microcontroller's memory [27]. Each value in the table determines the duty cycle of the IGBT. The timer0 is used as base frequency, defines the switching frequency, and was set at 7.8 kHz. Timer 1 reads the sine wave table, so when the count sequence is complete, a value of the sine table (turn-on time of the transistor) is loaded. Timer 1 defines the sine wave frequency, i.e. timer 1 determines which frequency will be used to read the sine table.

The trigger pulses from the microcontroller are driven to the transistor driver circuit. The trigger circuit enables the connection between the microcontroller and the semiconductor, providing a voltage of 15 V, which is necessary to start the IGBT. It also provides electrical isolation between the control stage and the power stage.

An IR2113 driver was used to turn on the transistors. Each driver can feed a branch of two IGBTs, feeding the top and the bottom semiconductor to create a floating point reference for

the upper driver. Trigger pulses for the different IGBTs are shown in Figure 7. While a pair of IGBTs is used to generate a half-cycle, the other pair remains off; roles are exchanged in the next half cycle.

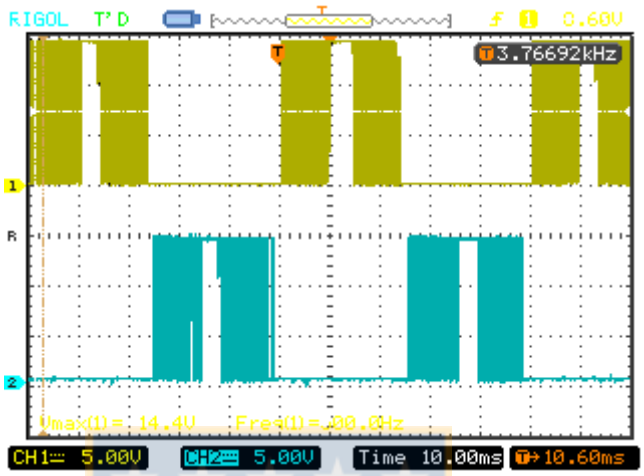

Figure 7. Driver circuit trigger pulses for IGBT 1 and 2 (top) and 3 and 4 (bottom).

Converter input signals correspond to the voltage and current in the DC link, the alternating voltage of the PMG and the input current to the pump. A LEM LV25-P cell was used as voltage sensor, while LEM HY 5 and HAS 50-S cells were used as current sensor. The current sensor in the pump allows tracking the electric current in order to ensure that it is within the operation range and prevent damage due to overheating of the IM.

Figure 8 shows the waveforms of the output voltage of the converter, and line current feeding the induction motor.

The harmonic content of voltage and current are shown in Figure 9. The predominant harmonics are around the switching frequency. Odd harmonics of small amplitude are close to the fundamental frequency.

The current is sinusoidal with amplitude of 5.2 Arms at 50 Hz and THD is 7.3%.

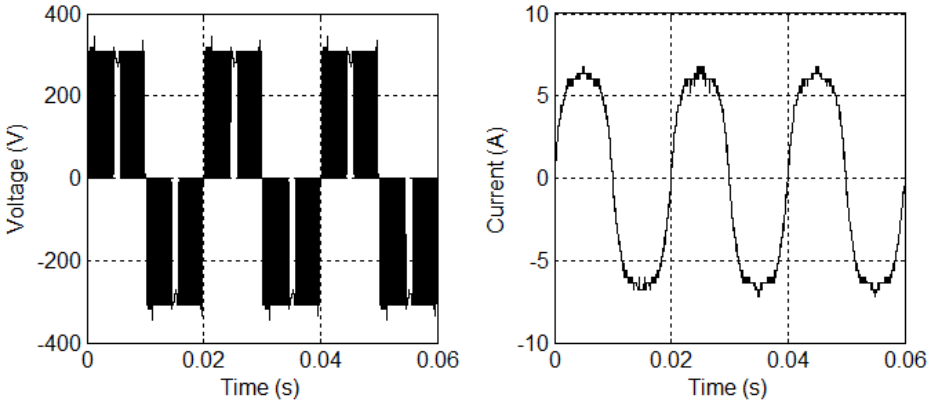

(a) (b)

Figure 8. Output voltage (a) and current (b) waveform feeding the IM.

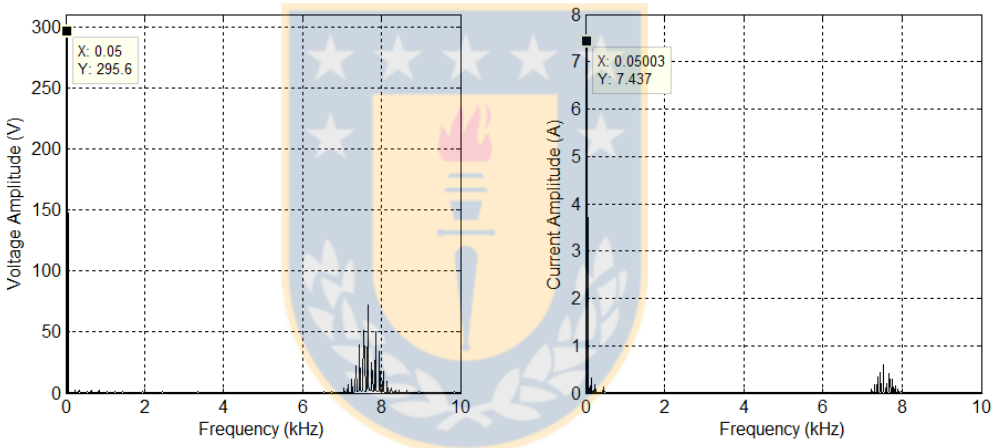

(a) (b)

Figure 9. Harmonic content of the voltage output of the inverter (a) and current (b).

Maximum power point tracking (MPPT)

The algorithm for maximum power point tracking controls the electrical frequency of the motor based on the power in the DC link. To accomplish this, it is necessary to count on the electrical power curve as a function of the generator rotational speed [28]. The electric power is determined by measuring the voltage and current in the DC link. Rotational speed is

determined by measuring the electrical frequency of the PMG, which are related to the number of poles. The maximum electrical power that the PMG should supply at that speed is obtained, which corresponds to the reference power for the control system. The reference power is compared with the DC value measured, and then the power consumed by the pump unit is adjusted by increasing or decreasing the electrical frequency of the inverter. A flowchart of this control algorithm is shown in Figure 10.

By altering the electrical frequency of the inverter, the rotational speed of the pump changes, which results in an increase or decrease in the power absorbed by the pump. In this way, a regulated load is applied to the generator by modifying the electrical power produced.

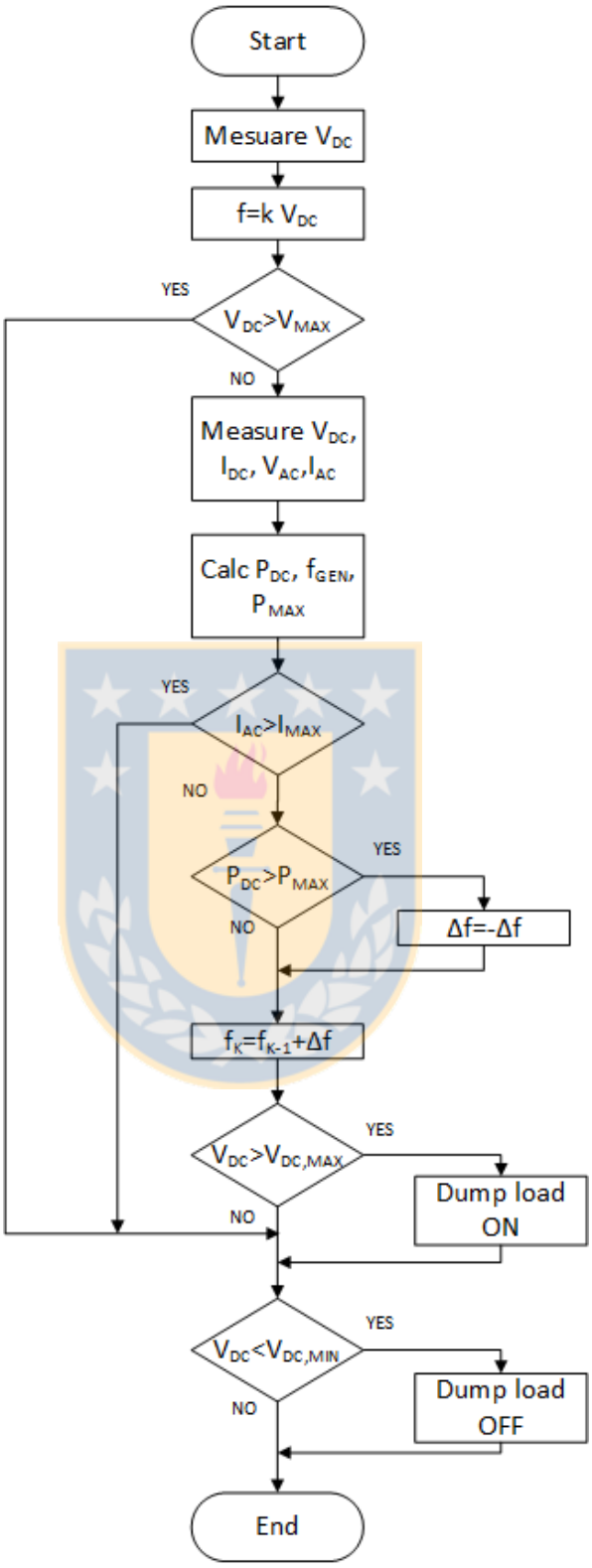

Figure 10. Flowchart of the control algorithm.

EXPERIMENTAL SETUP

In order to measure the efficacy of the converter, the configuration shown in Figure 11 was implemented in the laboratory. The mechanical power is provided by a three-phase induction motor fed from a variable frequency converter, which allows for rotational speeds throughout the operating range of the wind-electric pumping system. The operating point of the pump can be modified through a valve that regulates the flow and pressure at the output of the pump.

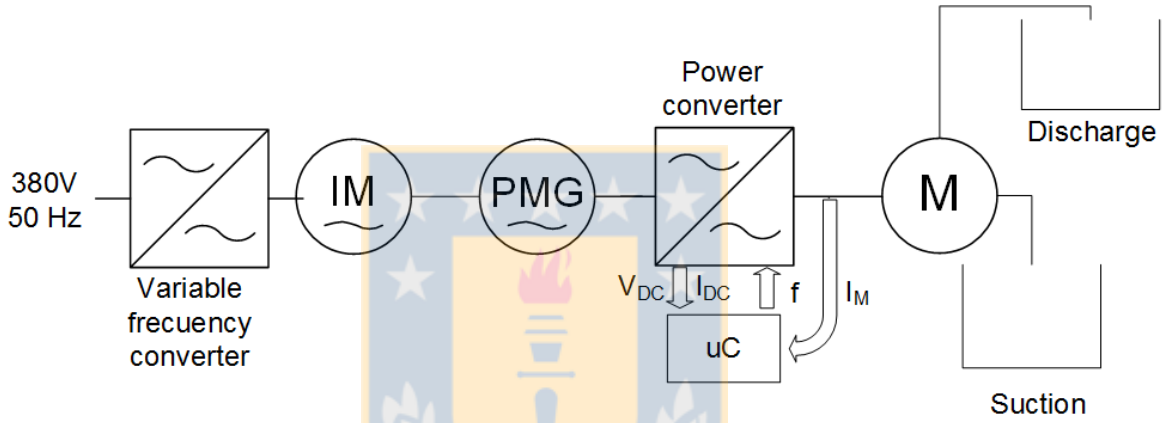

Figure 11. Test-bank for the power converter in the laboratory.

RESULTS

Electrical power generated by the PMG.

The generated electrical power was measured by modifying the pump operating point. By changing the pump outflow, the electric current absorbed by the pump is modified, causing a variation in the generated electric power while the rotational speed is kept constant. This process was conducted at different rotational speeds. The results obtained are shown in Figure 12.

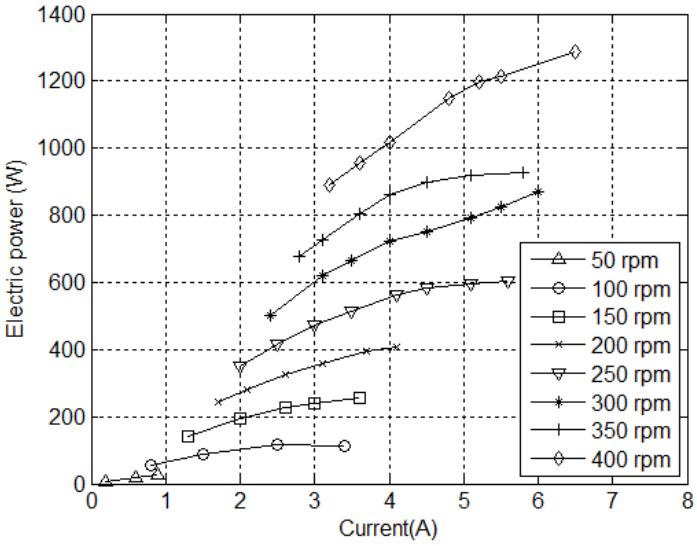

Figure 12. Electrical power generated at different rotational speeds of the PMG.

By increasing the current generated by the PMG, voltage drop increases in the impedance of the generator coils decreasing the generated voltage. Therefore, it is observed that the increase in power for the different rotational speeds is not linear, but curve. The maximum power supplied by the generator was 1,300 W.

Power converter performance

Measurements were done at different load levels to determine operating areas of the converter. To this end, the output pressure of the pump driven by converter was fixed at 10, 20, 25, 30, 40 and 50 m. Voltage on the DC link was also modified, between the minimum voltage required to start the pump (160 V) and the nominal voltage (311 V) of the system, changing the rotational speed of the PMG.

Two operational scenarios were established. In the first scenario, the control strategy of the power converter was set by keeping the V/f ratio constant. Therefore, the inverter frequency

was modified according to the changes in the DC link voltage in direct current seeking to operate at a flux magnitude roughly equal to the nominal flux. In the second scenario, the control strategy of the power converter was modified by taking the nominal V/f ratio of the motor as in the initial point, and then increasing the operational frequency of the converter. This results in an increased rotational speed of the pump and in a higher load for the system. Since, it is not possible to increase simultaneously voltage and frequency in the system, the pump motor works in a weak operational flux, which increases the motor slip and the current drawn. Because of this, this scenario has a restriction with the nominal value of the motor current, which is set to 5.0 A.

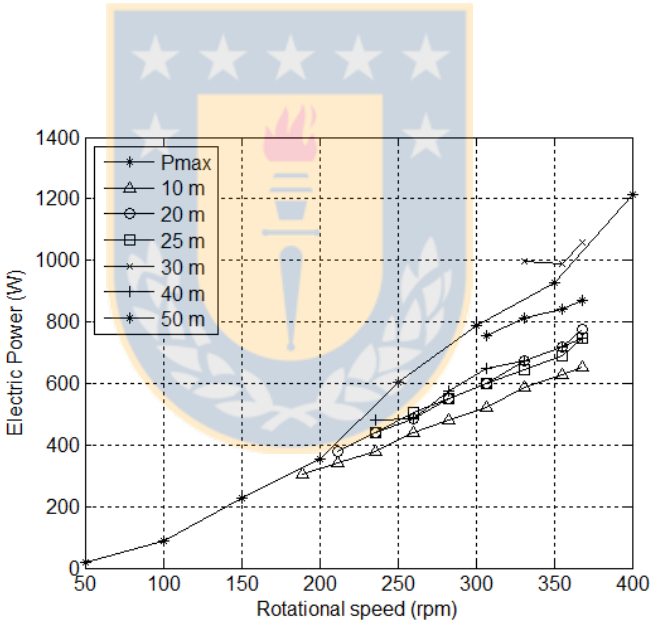

Figure 13. DC power variation at different electric loads for the V/f control strategy.

DC power curves for the V/f control strategy are shown in Figure 13. Maximum power in the link was 1,050 W, which occurs at the highest level of electric load, with the pump operating at nominal voltage and nominal current. It is observed that there are points above the maximum electrical power curve that cause an overload in the PMG.

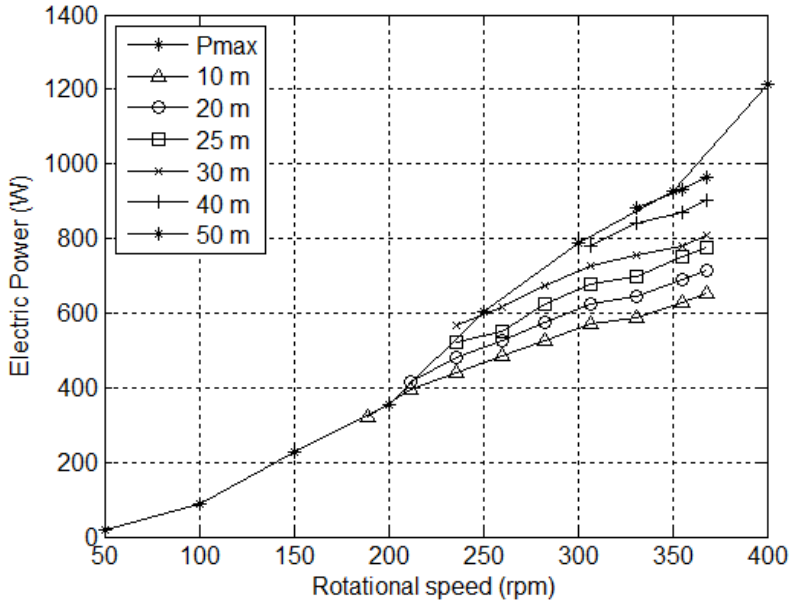

Figure14. DC power at different levels of electrical load for the V/f constant variable control strategy.

By operating with the MPPT strategy, an increase in the power generated by the PMG is obtained, as seen in Figure 14. An increase in power until reaching the current restriction of the IM is obtained at all levels of electric load measured. It is also observed that the overload is limited to the PMG, reaching power values that are lower or equal to the maximum electrical power. High or medium power levels result in a higher load for the generator, while nominal current of the motor is reached quickly at low levels. This restricts the maximum operating power because the IM is operating in a weak flow zone, which causes an increase in the motor slip and, thus, an increase in current.

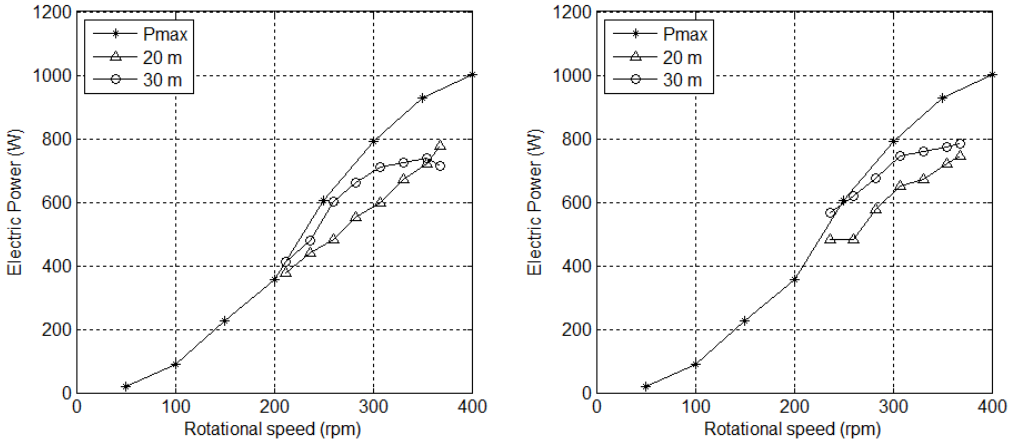

Figure 15. Comparison between two control strategies for a head 20 m and 30 m.

Figure 15 shows a comparison between the two control strategies for two load levels. It can be observed that there is an increase in the power in all measured points when using the MPPT control of the variable V/f ratio. This increase ranges between 19 and 136 W.

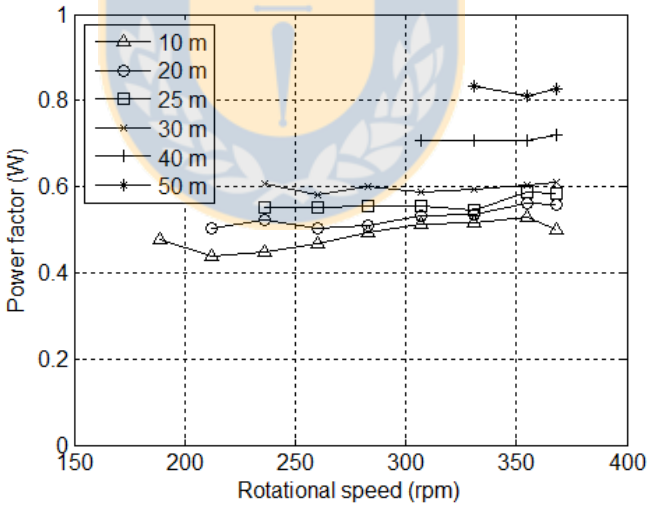

Figure 16. Variation in the power factor at different load levels.

Figure 16 shows the variations in the power factor of the pump. Power factor reaches a minimum value of 0.4 at minimum electrical load, in which the reactive component of the motor predominates, and a maximum value of 0.85 at maximum electrical load, in which the

active power predominates. Since the pump is driven by a power converter, there are power harmonics that decrease the effective operating power factor of the IM. The power factor can be improved using multilevel power converters that reduce harmonic contamination [29].

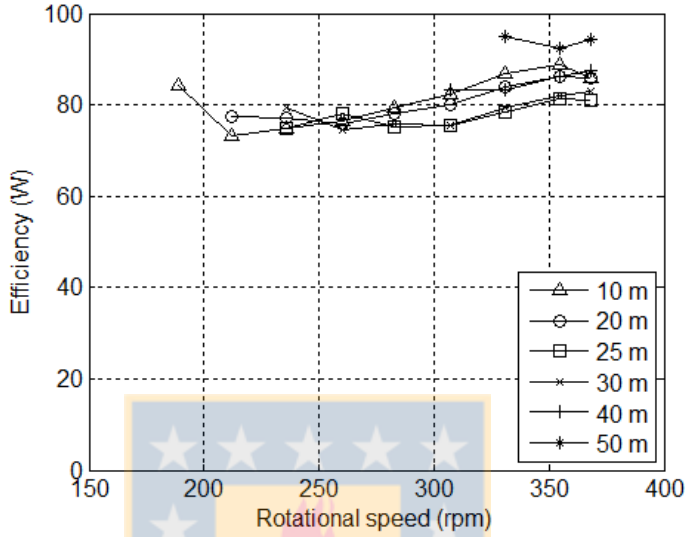

Figure 17. Variation of the converter's efficiency at different electrical loads.

As shown in Figure 17, converter efficiency ranges between 70% and 94% and it increases as load level is increased. This occurs because switching loss decreases comparatively with the power that is flowing through the converter. Moreover, switching losses increase at low operational electrical frequency because a larger number of switching is generated by the electrical cycle. The number of switching decreases as the electrical frequency increases.

CONCLUSIONS

A power converter with maximum power point tracking has been implemented for a wind-electric pumping system, which would prevent the use of batteries in a pumping system of low power. The power converter was tested and evaluated by analyzing the power range of the

system, the operation at variable rotational speed, the power developed for each control strategy and the efficiency of the converter.

Based on the measurements of power made in the experimental setup, a maximum power of 1,300 W was obtained for the greatest electrical load used in the pump. This value was obtained at a rotational speed of 350 rpm.

The IM was fed at variable voltage amplitude and frequency producing variable rotational speed. Rotational speed of the pump has a minimum value of 0.5 times the rated speed, which corresponds to half of the frequency and voltage of the motor with the minimum test load. As the pump load increases, more power is required to pump water, and thus the minimum speed at which water is pumped is higher and requires more voltage and frequency to start up.

Two strategies of control were implemented to allow the operation of the IM at different frequencies for different load levels. The control strategy with MPPT and variable V/f ratio allows for a greater factor of use for the PMG and an increased power absorbed by the pump for all load levels measured, compared to the nominal V/f ratio strategy. For medium to high load levels, the demanded electric power is close to the maximum power curve of the PMG, operating at maximum power in the case of the highest load level. Increased electrical power is limited by the nominal current of the pump motor in the other levels, and because of this, it is not close to the maximum power curve.

The efficiency achieved by the power converter implemented ranges from 70% to 95% depending on the operational load level of the pump. The power factor depends on the load of the pump and increases at higher load levels. The value of the power factor ranges between 0.4 and 0.85.

ACKNOWLEDGEMENTS

The authors would like to thank the financial support from the Ministry of Energy, FONDEF program (project D10ER1006), and the Vice-rectory of Research and Development of the University of Concepción (project VRID 212.131.015-1.0).

REFERENCES

[1] IEEE, “IEEE Recommended Practice for Sizing Lead-Acid Batteries for Stand-Alone Photovoltaic (PV) Systems.” 2010.

[2] B. D. Vick, R. N. Clark, and P. O. Drawer, “Testing of a 2-kilowatt wind-electric system for water pumping,” *AWEA Wind.*, 2000.

[3] D. D. Lara, G. G. Merino, B. J. Pavez, and J. A. Tapia, “Efficiency assessment of a wind pumping system,” *Energy Convers. Manag.*, vol. 52, no. 2, pp. 795–803, 2011.

[4] R. N. Clark and B. Vick, “Determining the proper motor size for two wind turbines used in water pumping,” *Wind Energy 1995*, pp. 65–72, 1995.

[5] E. Muljadi, G. Nix, and J. T. Bialasiewicz, “Analysis of the dynamics of a wind-turbine water-pumping system,” in *Power Engineering Society Summer Meeting, 2000. IEEE*, 2000, vol. 4, pp. 2506 –2519 vol. 4.

[6] M. S. Miranda, R. O. C. Lyra, and S. R. Silva, “An alternative isolated wind electric pumping system using induction machines,” *Energy Conversion, IEEE Trans.*, vol. 14, no. 4, pp. 1611–1616, 1999.

[7] T. Ouchbel, S. Zouggar, M. L. Elhafyani, M. Seddik, M. Oukili, a. Aziz, and F. Z. Kadda, “Power maximization of an asynchronous wind turbine with a variable speed feeding a centrifugal pump,” *Energy Convers. Manag.*, vol. 78, pp. 976–984, Feb. 2014.

[8] J. S. Anagnostopoulos and D. E. Papantonis, “Pumping station design for a pumped-storage wind-hydro power plant,” *Energy Convers. Manag.*, vol. 48, no. 11, pp. 3009–3017, Nov. 2007.

[9] R. D. Fernandez, R. J. Mantz, and P. E. Battatotto, “Sliding Mode Control for Efficiency Optimization of Wind Electrical Pumping Systems,” *Wind Energy*, vol. 6, no. 2, pp. 161–178, 2003.

[10] B. D. Vick and R. N. Clark, “Performance of wind-electric and solar-PV water pumping systems for watering livestock,” *Trans. Soc. Mech. Eng. J. Sol. ENERGY Eng.*, vol. 118, pp. 212–216, 1996.

[11] D. Fiaschi, R. Graniglia, and G. Manfrida, “Improving the effectiveness of solar pumping systems by using modular centrifugal pumps with variable rotational speed,” *Sol. Energy*, vol. 79, no. 3, pp. 234–244, 2005.

[12] A.-K. Daud and M. M. Mahmoud, “Solar powered induction motor-driven water pump operating on a desert well, simulation and field tests,” *Renew. Energy*, vol. 30, no. 5, pp. 701–714, 2005.

[13] A. M. De Broe, S. Drouilhet, and V. Gevorgian, “A peak power tracker for small wind turbines in battery charging applications,” *Energy Conversion, IEEE Trans.*, vol. 14, no. 4, pp. 1630–1635, 1999.

[14] I. Schiemenz and M. Stiebler, “Control of a permanent magnet synchronous generator used in a variable speed wind energy system,” in *Electric Machines and Drives Conference, 2001. IEMDC 2001. IEEE International*, 2001, pp. 872–877.

[15] A. B. Raju, K. Chatterjee, and B. G. Fernandes, “A simple maximum power point tracker for grid connected variable speed wind energy conversion system with reduced switch count power converters,” in *Power Electronics Specialist Conference, 2003. PESC ’03. 2003 IEEE 34th Annual*, 2003, vol. 2, pp. 748 – 753 vol.2.

[16] E. Koutroulis and K. Kalaitzakis, “Design of a maximum power tracking system for wind-energy-conversion applications,” *Ind. Electron. IEEE Trans.*, vol. 53, no. 2, pp. 486–494, 2006.

[17] W.-M. Lin and C.-M. Hong, “Intelligent approach to maximum power point tracking control strategy for variable-speed wind turbine generation system,” *Energy*, vol. 35, no. 6, pp. 2440–2447, Jun. 2010.

[18] D. Bang, H. Polinder, G. Shrestha, and J. A. Ferreira, “Review of generator systems for direct-drive wind turbines,” in *European Wind Energy Conference & Exhibition, Belgium*, 2008, pp. 1–11.

[19] G. Inc., “PMG1600.” [Online]. Available: www.ginglong.com.

[20] T. Ouchbel, S. Zouggar, M. L. Elhafyani, M. Seddik, M. Oukili, A. Aziz, and F. Z. Kadda, “Power maximization of an asynchronous wind turbine with a variable speed feeding a centrifugal pump,” *Energy Convers. Manag.*, vol. 78, pp. 976–984, Feb. 2014.

[21] E. R. Collins, “Torque and slip behavior of single-phase induction motors driven from variable frequency supplies,” in *Conference Record of the 1990 IEEE Industry Applications Society Annual Meeting*, 1990, pp. 61–66.

[22] D. Yildirim and M. Bilgic, “PWM AC chopper control of single-phase induction motor for variable-speed fan application,” *Industrial Electronics, 2008. IECON 2008. 34th Annual Conference of IEEE*. pp. 1337–1342, 2008.

[23] A. Z. Latt and N. N. Win, “Variable Speed Drive of Single Phase Induction Motor Using Frequency Control Method,” *Education Technology and Computer, 2009. ICETC ’09. International Conference on*. pp. 30–34, 2009.

[24] S. B. Kjaer, J. K. Pedersen, and F. Blaabjerg, “A Review of Single-Phase Grid-Connected Inverters for Photovoltaic Modules,” *IEEE Trans. Ind. Appl.*, vol. 41, no. 5, pp. 1292–1306, Sep. 2005.

[25] L. Clotea, A. Forcos, C. Marinescu, and M. Georgescu, “Power losses analysis of two-level and three-level neutral clamped inverters for a wind pump storage system,” *Optim. Electr. Electron. Equip. (OPTIM), 2010 12th Int. Conf.*, pp. 1174–1179, May 2010.

[26] B. Ismail, S. Taib, A. R. M. Saad, M. Isa, and C. M. Hadzer, “Development of a Single Phase SPWM Microcontroller-Based Inverter,” in *2006 IEEE International Power and Energy Conference*, 2006, pp. 437–440.

[27] A. A. Qazalbash, A. Amin, A. Manan, and M. Khalid, “Design and implementation of microcontroller based PWM technique for sine wave inverter,” in *2009 International Conference on Power Engineering, Energy and Electrical Drives*, 2009, pp. 163–167.

[28] R. Kot, M. Rolak, and M. Malinowski, “Comparison of maximum peak power tracking algorithms for a small wind turbine,” *Math. Comput. Simul.*, vol. 91, pp. 29–40, May 2013.

[29] Feel-Soon Kang, Sung-Jun Park, Han-Woong Park, and Cheul-U Kim, “A novel high performance single-phase 3-level PWM inverter,” in *ISIE 2001. 2001 IEEE International Symposium on Industrial Electronics Proceedings (Cat. No.01TH8570)*, 2001, vol. 2, pp. 922–927.

Paper III

Performance of pumps operated at variable speed in a direct-coupled wind pumping system

by

David Lara, Gabriel Merino, Luis Lagos

Performance of pumps operated at variable speed in a direct-coupled wind pumping system

David Lara, Gabriel Merino, Luis Lagos

ABSTRACT

Wind-electric water pumping systems operate under temporal fluctuations in wind speed that cause variations in electric power. This results in the pump operating under fluctuating power and at variable rotational speed. The use of power converters allows regulating rotational speed by control algorithms. The objective of this work was to evaluate the hydraulic performance of two different types of pumps: peripheral 746 W and centrifugal 600 W in a wind-electric pumping system at variable speed. The effect of operating with a linear V/f ratio and a variable V/f ratio was also evaluated. The peripheral pump can pump water at a slower rotational speed than the centrifugal pump under various pump pressures, reaching up to 1,636 rpm for a pressure of 20 m, 600 rpm lower than the operating speed achieved by the centrifugal pump. The variable V/f control developed higher rotational speeds than the linear V/f; flow rates increased 17% for pressures from 20 to 30 m. Field tests shows that the system can pump at rated operating conditions, reaching values of up to 40 L min^{-1} for a static height of 11 m.

INTRODUCTION

Irrigation systems have traditionally used only conventional energy sources, such as electric power and power generators. However, new types of energy have been introduced in recent years, so that non-conventional renewable energy sources (NCRE), such as wind power and photovoltaic energy (PV), are also being used.

Wind and PV pumping systems are especially suitable for supplying water in isolated locations of the network [1]. However, due to the continuous rise of electricity prices, small power systems are being installed in order to reduce operating costs.

Regarding irrigation, the standard configurations of pumping systems that use renewable energy do not include direct coupling between aerogenerators or photovoltaic modules and pumps, which requires the use of batteries for energy storage. This results in higher costs and problems associated with operation and maintenance of the system [2].

Systems with battery bank are able to maintain voltage constant, allowing the use of pumps with electric power supply with similar characteristics to the network (220 o 380V/ 50 Hz) by using a voltage inverter. Therefore, selection of the pump irrigation system is performed considering the characteristics of the site [3], and determining the operating point pressure (H) - flow rate (Q) of the irrigation system, which is obtained by intersecting the H - Q system curve with the pump characteristic curve [4].

Power output is variable in systems without battery banks and it is not possible to maintain pressure and flow rate constant. Therefore, pumps are operated at variable rotational speed according to fluctuations in power supply.

Direct-coupled PV systems have been widely applied to water pumping systems, mainly because solar radiation has less temporal variability than wind speed. PV systems offer higher reliability and have greater economic feasibility compared to diesel-powered systems [5]. They can also provide high availability of water without storing energy in batteries [6]. Their use and economic operation [7] have been optimized so that different systems for maximum power point tracking (MPPT) have been developed, controlling the voltage and current generated regardless of the load [8]. Different types of pumps are used in these systems, such as volumetric and screw pumps, or centrifugal pumps, which are more widely used [6].

In wind electric pumping systems without battery bank, the electrical power generated goes directly to the pump or through a power converter, and the pumped water is stored in a tank. Continuous fluctuations of power generation occur, which affects the rate of rotation of the pump and results in different operating points, unlike what occurs when power is fed from the electrical grid.

This configuration of wind-electric pumping systems has been mainly used as energy storage system for the integration of wind power to the grid at high power. However, it can also be used in low-power integrated systems [9].

Low-powered wind pumping systems have been implemented in powers from 0.5 kW to 10 kW and are used for pumping water for domestic and livestock use [10]. During decades, Clark and Vick of the United States Department of Agriculture (USDA) - Agricultural Research Service have conducted studies that include the windmill [11],[12] and wind-electric pumping systems in which a permanent magnet generator (PMG) is directly coupled to a standard pump [13]. Direct-coupled systems have been tested in different configurations of wind-electric pumping [14], [15]. Electronic control systems that increase the power captured

by the turbine [16] have been developed , also incorporating improved aerodynamic profiles of wind turbines [17].

Since, in direct-coupled systems, the motor operates the pump at variable speed, the pumping features are modified. The motor's admissible rotational speeds can decrease up to 20% of its rated speed. However, a decrease in speed is determined by the water pumping capacity, reaching an estimated range between 60% and 110% of the rated speed [18], which depends on the local characteristics of water pumping and pump type.

The selection of a pump for a direct-coupled wind-electric pumping system cannot be approached using the procedure described before because the characteristic curves that specify the operation of the pumps are not enough to select a pump operating at variable rotational speed. Therefore, it is necessary to determine the behavior of the pumps at speeds other than those provided in the data sheet of the manufacturer in order to determine the fluctuations in pressure and flow rate, and based on this determine the range in which the pump works effectively for a direct-coupled wind-electric pumping system with a power converter.

This work focuses on the evaluation of two types of commonly used pumps, centrifugal and peripheral, operating at variable rotational speed in a direct-coupled wind-electric pumping system with a power converter. The objective is to determine which type of pump is more suitable for the pumping system based on the amount of pumped water and the working range of the rotational speed. The effect of operating with a MPPT will also be evaluated based on the amount of water pumped.

Pump operation at variable rotational speed

The hydraulic performance of a pump is specified by its characteristic curve, which describes the relationship between the flow rate and pressure developed by the pump. This curve is complemented with power consumption curves, NPSH (Net Positive Suction Head) curves, and occasionally with yield curves, depending on the flow rate and for a given rotational speed [4].

The pressure curve (H_m) versus flow rate (Q) can be expressed, in general, by a quadratic equation, as follows:

$$H_m(Q) = aQ^2 + bQ + c \quad (1)$$

Coefficients a, b and c can be calculated with three points of the curve or by adjusting the curve. The pump curve is obtained by plotting the Equation (1), as shown in Figure 1.

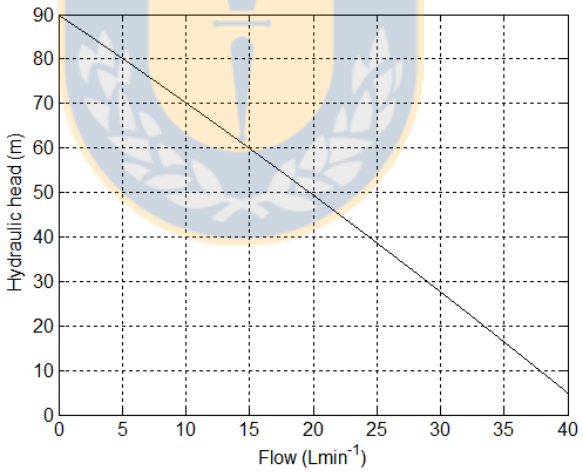

Figure 1. Curve adjustment for pump pressure – flow rate at rated rotational speed.

The operation of electric pumps at variable speed can be theoretically described by the affinity laws. These laws express the relationship between flow rate Q, pressure H and power

consumption P as a function of the rotational speed n, assuming that pump efficiency remains constant [19].

$$\frac{Q_2}{Q_1} = \frac{n_2}{n_1}$$
$$\frac{H_2}{H_1} = \frac{n_2^2}{n_1^2} \quad (2)$$
$$\frac{P_2}{P_1} = \frac{n_2^3}{n_2^3}$$

When applying these relations to an operating point H_1 - Q_1 at a known rotational speed, it is possible to obtain the operating point H_2 – Q_2 at another rotational speed. Thus, it is possible to produce, in theory, different characteristic curves H - Q at different rotational speeds, as shown in Figure 2.

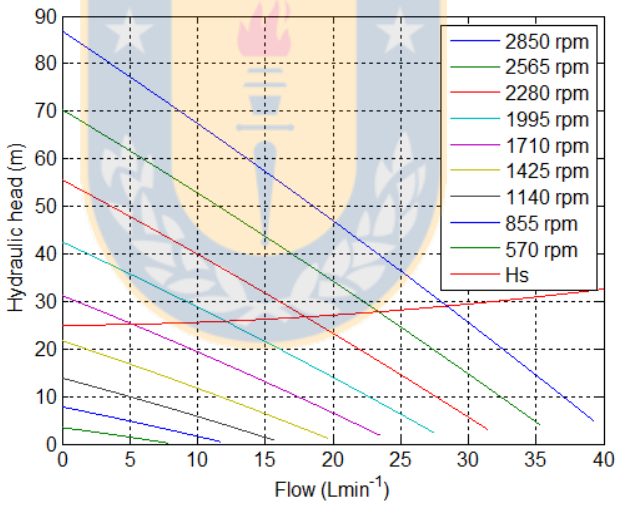

Figure 2: Family of characteristic curves H-Q obtained from pump data and affinity laws and the system load curve (H).

Furthermore, static pumping height and all components of the water drive system generate the pressure - flow rate relationship of the system, as described by equation (3):

$$H_s(Q) = H_T + \sum h_f + \sum h_m \quad (3)$$

Where H_s is the total dynamic pressure, H_T the static height, h_f represents frictional losses in the pipes and h_m represents singularity losses. Friction losses h_f can be calculated using the Darcy-Weibach equation [20].

As both frictional and singularity losses are proportional to the square of flow speed, the characteristic pressure of the water lift system has a quadratic increase with the flow rate, as shown in Figure 2.

The pump operation points correspond to the intersection of the water lift system curve and the characteristic pump curve. When reducing the rotational speed of the pump, both the flow and pressure decrease, and the operation point decreases at a lower flow rate and pressure. There is a minimum rotational speed at which the pressure exerted by the pump slightly exceeds the system pressure to obtain a minimum flow extracted. At lower rotational speeds, no flow rate is obtained.

As there are many different types of pumps, and pumping conditions vary depending on the place, it is necessary to determine what type of pump can deliver a greater volume of water under certain pumping conditions.

EXPERIMENTAL SETUP

In order to select a suitable pump for a wind-electric pumping system, pumps were tested at variable speed in the laboratory and a prototype system of a wind-electric pumping with a power converter was implemented (Figure 3).

To experimentally determine the pressure-flow relationship in a pump operated at rotational speeds other than the rated speed, a test setup was implemented consisting of: a frequency inverter to operate the pump motor at different rotational speeds and the pump being tested.

Pipe outlet pressure was measured with a manometer C830402K with an accuracy of up to ±0.5% at full scale. A flowmeter, model F-2000 (Blue-White Industries) with accuracy at full scale was used to determine flow rate. The rotational speed of the pump was measured with a contact tachometer, model DT-2236 (Lutron electronics), with an accuracy of±0.01%. A flow rate control valve was used to regulate flow rate and pressure.

Additionally, the electrical power required by the pump motor was measured using an oscilloscope Rigol DS1052E.

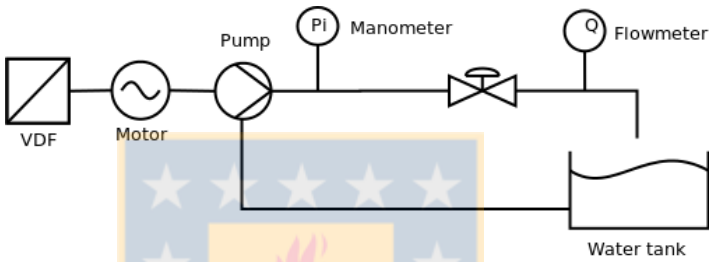

Figure 3. Experimental Setup for the measurement of pump characteristic curves.

A centrifugal pump and a peripheral pump, which are commonly used in low power irrigation systems, were tested. Technical data of these pumps are shown in Table 1.

Table 1. Technical data of the pumps

	Peripheral pump	Centrifugal pump
Power (W)	600	746
Voltage (V)	230	230
Current (A)	5.2	6.0
Rated speed (rpm)	2900	2900
Max. pressure (m)	65	36
Max. flow rate($Lmin^{-1}$)	50	90

After evaluating the performance of the two pumps at variable speed, the pump that exhibited a better performance in operation was used in the wind-electric pumping system. A layout of this system is shown in Figure 4. The system consists of a permanent magnet generator (PMG) of 1.3 kW, a power converter and the pump, which is driven by a single-phase induction motor (IM). The water was pumped into a pool, while flow rate and pressure were regulated through a throttle valve. The PMG is driven by a variable frequency drive and a three-phase IM, which provided mechanical power throughout the working speed interval of the PMG.

The power converter has a microcontroller that can be programmed with different control strategies. Two control strategies were compared in order to determine if there was an increase in the amount of water pumped to each. The first strategy corresponds to the linear V/f ratio, and the second corresponds to a MPPT with variable V/f ratio, which changes the frequency of the power converter and, consequently, the rotational speed of the pump.

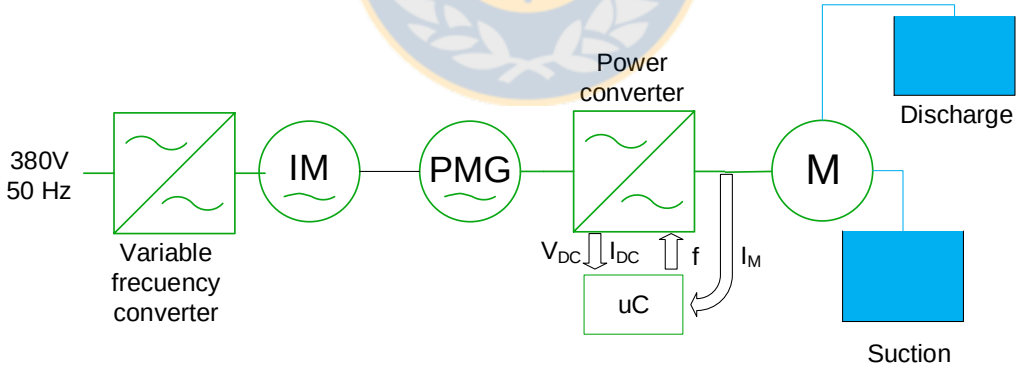

Figure 4. Test-bank for the power converter in the laboratory.

Finally, the prototype of the wind-electric pumping system was installed in the field. A three-bladed turbine of 2 meters of radio, designed with a NACA 4412 airfoil profile for a rotational

speed of 380 rpm at a wind speed of 9 m s^{-1}, was coupled to the PMG. The turbine was installed in a tubular tower of 14 m high. The system pumps water from a tank to a height of 11 m. This static height can provide sufficient pressure for drip emitters operating from 5 to 10 m.

Wind speed data were obtained with a Decagon anemometer and a wind vane, with a resolution of 0.45 m s^{-1} and 1° for wind speed and direction, respectively. Data were recorded every 1 minute and were stored in a DEC-EM50 data logger (Decagon Device). A data acquisition system (DAS) was implemented to measure the flows of electric power in the system, the pressure and flow rate. LV-25P voltage sensors in the DAS were used and the LEM HAS 50S cell was used for the currents. These sensors were installed in the PMG, DC link and IM. The analog output of the F2000 flowmeter was used to estimate flow rate, while the transducer's an analog output was used to measure pressure (4-20 mA). All signals were conditioned and transferred to the Arduino Mega 2560 microcontroller. Values of electrical power, pressure and flow were calculated every minute. This enabled to determine the flow rate of water pumped for each wind speed.

RESULTS

Pump performance at variable speeds.

The pumps were operated in the frequency range from 20 to 50 Hz by a frequency inverter that allowed developing rotational speeds between 1,145 rpm and 2,790 rpm. The flow rate and outlet pressure were controlled by a throttle valve from zero to rated flow, achieving H–Q operation points at different rotational speeds for each pump.

Figure 5 shows the results obtained for the peripheral pump. It is observed that pressure decreases at a greater rate than flow when decreasing the rotational speed. This occurs because of the quadratic pressure dependence on rotational speed. The minimum pressure recorded was 14 m at a rotational speed of 1,145 rpm, in which the flow was almost zero.

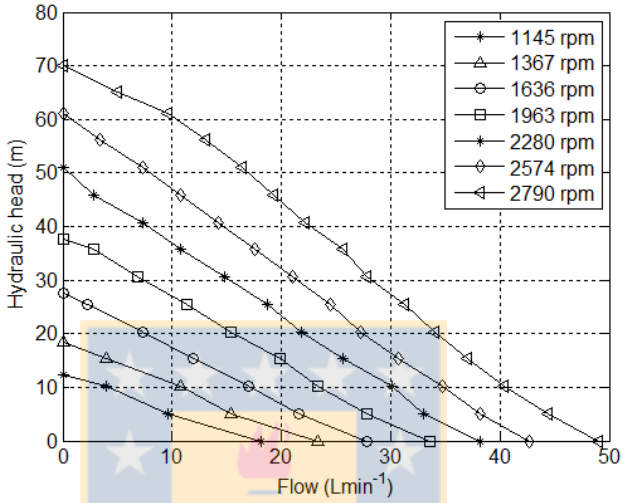

Figure 5. Family of H-Q curves for the peripheral pump.

Figure 6 shows the results obtained for the centrifugal pump. In this case, the minimum pressure achieved was 5 m at a rotation speed of 1,182 rpm with a minimum flow rate of operation. Given the nature of the pump flow pressure, the operating pressure was lower compared to the one recorded in the peripheral pump.

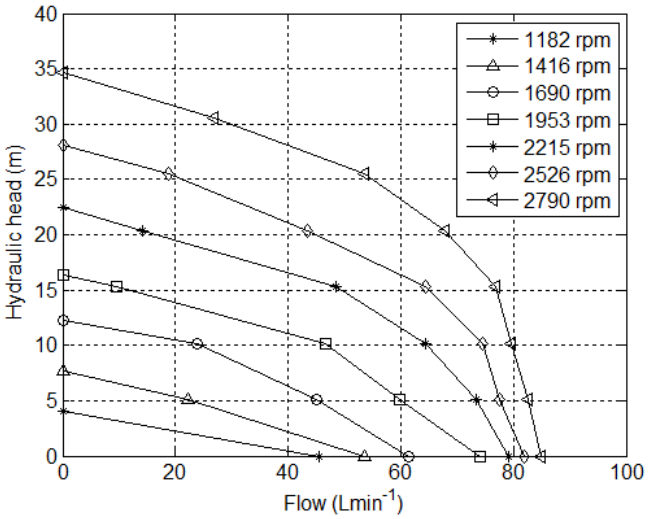

Figure 6. Family of H-Q curves for the centrifugal pump.

When comparing the rotational speeds of these pumps, it is observed that the peripheral pump can be driven at a lower frequency than the centrifugal pump, and still obtain a small but existing water flow.

The difference in operating frequency is not critical at low operating pressures, below 10 m, but it is at higher pressures. For example, with a pumping pressure of 25 m, a centrifugal pump will draw water only until a frequency near 40 Hz, producing rotational speeds of about 2,215 rpm, while a peripheral pump will do it until 30 Hz, that is, at rotational speeds of about 1,690 rpm. This allows a higher operating speed range for the peripheral pump.

Therefore, pumps with a characteristic curve $H - Q$ of a pronounced slope, that is, exhibiting a wide pressure range at different flow rates, are suitable for operation at variable speeds because they can draw water at a greater range of rotational speeds, especially at reduced speeds.

Pump performance in a wind-electric pumping system

The peripheral pump was installed in the wind-electric pumping system and it was powered by a power converter. The power converter was made up of a 6-pulse rectifier, a capacitor bank and a single-phase H-bridge inverter. The drive control unit was programmed with the two algorithms: the linear V/f control and the MPPT algorithm of variable V/f ratio.

The linear V/f control takes advantage of the PMG voltage, which increases in amplitude as rotation of speed increases. The DC rectified voltage is used as a reference for the inverter, modifying the frequency according to voltage variations. Finally, the rotational speed of the pump will depend on the magnitude of the DC voltage, the electrical frequency generated by the inverter and the hydraulic load to be carried.

The variable V/f control was implemented in order to increase the electrical output generated, following the maximum power characteristic of the PMG. In order to adjust the operating power to the maximum power, the rotational speed of the PMG was modified by changing the electrical load. Changes in the electrical load were obtained by increasing or decreasing the electrical frequency using an inverter. Since the voltage remains constant during changes in frequency, the IM works mainly under magnetic flux weakening conditions.

By changing the electrical frequency, the rotational speed of the electric pump is modified. This causes an increase or decrease in the power absorbed by the pump so that the electrical load required by the PMG is regulated by adjusting the electrical power generated.

Table 2 shows the rotational speeds measured in the pump at steady-state. Data correspond to the peripheral pump at different pressures of the pumping system for both control strategies. It is observed that when operating with a variable V/f control strategy, there was an increase in the rotational speed in all of the cases when compared to the linear V/f control. This means

that there is an increase in the power generated by the PMG and that absorbed by the pump. This increase in pump power is also reflected in the hydraulic power. The zero values in the Table 2 represent pumping pressures that are not possible to achieve for the power generated by the PMG.

Table 2. Comparison between rotational speeds developed for each type of control with different voltage levels in the converter V_{DC}.

Rotational speed (rpm)												
	Linear V/f control						Variable V/f control					
V_{DC}	**10 (m)**	**20 (m)**	**25 (m)**	**30 (m)**	**40 (m)**	**50 (m)**	**10 (m)**	**20 (m)**	**25 (m)**	**30 (m)**	**40 (m)**	**50 (m)**
160	1464	0	0	0	0	0	1493	0	0	0	0	0
180	1644	1610	0	0	0	0	1737	1807	0	0	0	0
200	1835	1821	1780	1818	0	0	1915	2003	1935	2066	0	0
220	2010	1990	1916	1922	0	0	2062	2189	2129	2280	0	0
240	2224	2116	2162	2141	0	0	2301	2328	2457	2490	0	0
260	2400	2381	2368	2322	2223	0	2529	2619	2574	2691	2362	0
280	2582	2590	2578	2534	2438	2340	2605	2907	2802	2872	2590	2434
300	2784	2760	2710	2688	2623	2530	2809	3230	3011	3055	2730	2631
311	2873	2868	2861	2794	2732	2623	2873	3356	3179	3175	2965	2728

Variations in the rotational speed of the pump change the pump operating point and result in flow variations. As the speed of rotation of the pump increased, a shift in its operating point towards a higher flow was observed.

Figure 7 shows the difference between the pumped flow using the variable and linear V/f controls. The largest increases occurred in the area close to the system rated voltage, with increases of 6 L min^{-1}, 3 L min^{-1}, 4 L min^{-1} and 2 L min^{-1} for each of the tested pressures.

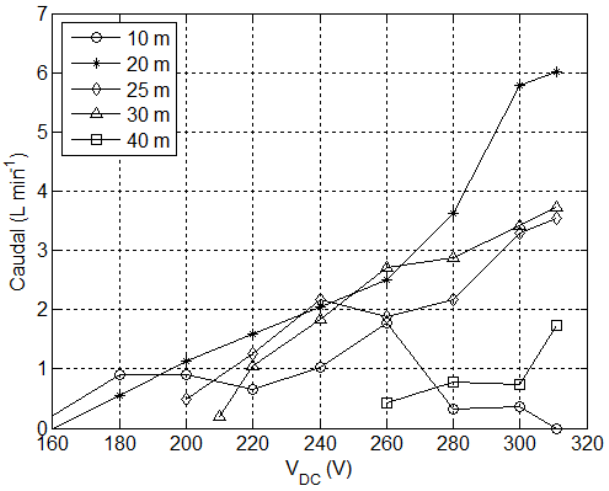

Figure 7. Differences between pumped flows using different converter control strategies.

In-field assessment of the wind-electric pumping system

Data of wind speed data and pumping system variables were ranked according the magnitude of wind speed using the interval method. Data were classified in intervals of 0.5 m s^{-1} in width, centered at multiples of 0.5 m s^{-1}; mean values for wind speed and power for each interval were obtained according to the following equations:

$$V_i = \frac{1}{N_i} \sum_{j=1}^{N_i} V_{i,j} \quad (4)$$

$$P_i = \frac{1}{N_i} \sum_{j=1}^{N_i} P_{i,j} \quad (5)$$

Where:

V_i : Mean wind speed in an interval *i*.

$V_{i,j}$: Measured wind speed *j*, in an interval *i*.

P_i : Electric power output in an interval *i*.

$P_{i,j}$: Measured power output *j*, in an interval *i*.

N_i : Number of data values in an interval *i*.

The curve of the average power generated in each interval is shown in Figure 8. The range of measured wind speeds reached up to 10.5 m s^{-1}. Higher values of wind speed were recorded, but these did not have sufficient time duration to be analyzed. The pumping system began operating at a wind speed of 3 m s^{-1}, and it was possible to measure up to 550 W of average power.

Figure 9 shows the average rotational speed of the wind turbine in each interval. The increase in the rotational speed was proportional to the incident wind speed up to about 8 m s^{-1}, reaching 330 rpm. At higher rotational speeds, power dissipation mechanisms are activated, so that power stops increasing directly with wind speed. The maximum speed recorded was approximately 374 rpm.

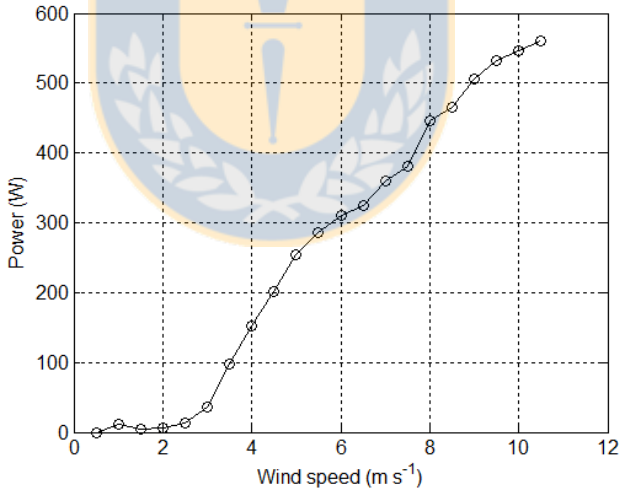

Figure 8. Curve of mean power generated for the wind-electric pumping system at a static pumping height of 11 m.

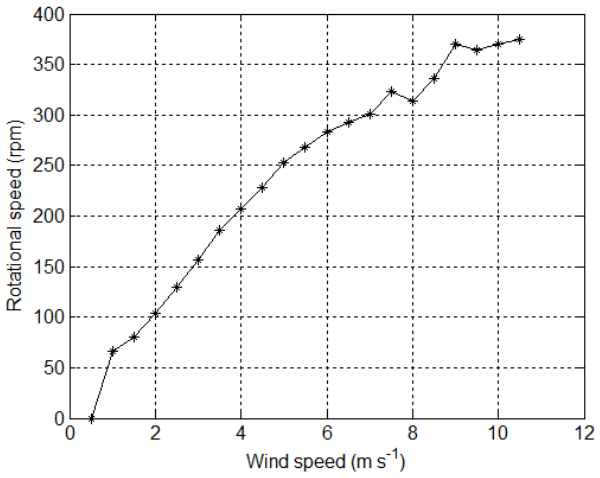

Figure 9. Mean rotational speed of the wind turbine.

The procedure already described for the wind data was used to determine the flow curve of the pumping system versus wind speed, also using the interval method. The flow corresponding to a given wind speed was determined from the following equation:

$$Q_i = \frac{1}{N_i} \sum_{j=1}^{N_i} Q_{i,j} \quad (6)$$

Q_i : Mean flow in an interval *i*.

$Q_{i,j}$: Measured flow *j*, in an interval *i*.

N_i : Number of data values in an interval *i*.

Flow measurements are shown in Figure 11. It can be observed that at a wind speed of 2.5 m s^{-1}, there is a constant increase of water pumped with wind speed. The flow rate is lower from 8 m s^{-1}, reaching a maximum value of around 40 L min^{-1}.

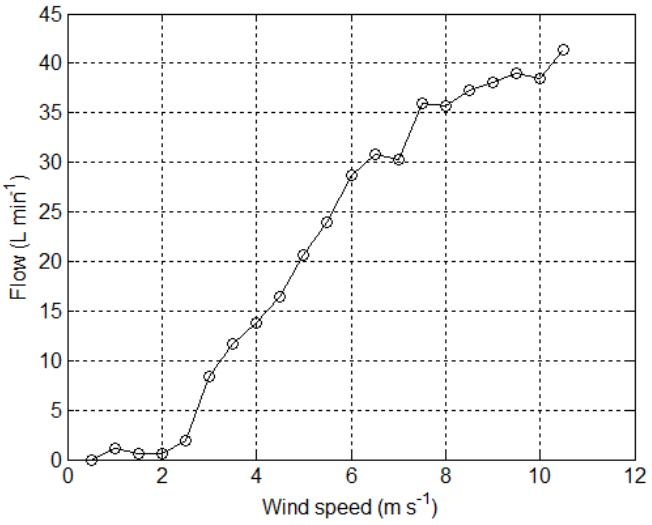

Figure 10. Mean flow pumped at different wind speeds.

CONCLUSIONS

Two types of pumps, centrifugal and peripheral, were evaluated in order to determine which of them is suitable for a direct-coupled wind-electric pumping system at variable speed, using a power converter.

By operating the pumps at variable speed, *H-Q* operating characteristics were obtained for rotational speeds other than rated speed. Pressure decreases quadratically with rotational speed, while flow rate decreases linearly. Results indicate that at the minimum rotational speed for a pressure of 20 m, the centrifugal pump delivers water up to 2,215 rpm, while the peripheral does it up to 1,636 rpm. For all the pump pressures tested, the peripheral pump had lower rotational speeds. This means that the wind pumping system operates with lower wind speeds, and, consequently, with a lower wind power.

The behavior of the peripheral pump in the wind pumping system was analyzed by programming two types of controls in the power converter. Speeds developed by the variable

V/f control were higher than those developed by the linear V/f control, with a consequent increase in the flows pumped. The highest flow increase was recorded for pumping pressures between 20 and 30 m, reaching up to 17%. The increase in flow was lower at the extreme operating pressures of 10 and 40 m, recording an 8% increase.

The field test shows that the system can pump water from a wind speed of 2.5 m s^{-1}, reaching a rate of 40 L min^{-1} for rated wind speed.

ACKNOWLEDGEMENTS

The authors would like to thank the financial support from the Ministry of Energy, the FONDEF program (project D10ER1006), and the Vice-rectory of Research and Development of the University of Concepción (project VRID 212.131.015-1.0).

REFERENCES

[1] G. G. Merino, L. O. Lagos, and J. E. Gontupil, "Monitoring and evaluation of a direct coupled photovoltaic pumping system," *Appl. Eng. Agric.*, vol. 24, no. 3, pp. 277–284, 2008.

[2] D. D. Lara, G. G. Merino, B. J. Pavez, and J. a. Tapia, "Efficiency assessment of a wind pumping system," *Energy Convers. Manag.*, vol. 52, no. 2, pp. 795–803, Feb. 2011.

[3] K. MEAH, S. ULA, and S. BARRETT, "Solar photovoltaic water pumping—opportunities and challenges," *Renew. Sustain. Energy Rev.*, vol. 12, no. 4, pp. 1162–1175, May 2008.

[4] E. Larralde and R. Ocampo, "Pump selection: a real example," *World Pumps*, vol. 2010, no. 3, pp. 28–33, 2010.

[5] A.-K. Daud and M. M. Mahmoud, "Solar powered induction motor-driven water pump operating on a desert well, simulation and field tests," *Renew. Energy*, vol. 30, no. 5, pp. 701–714, 2005.

[6] A. Hamidat and B. Benyoucef, "Systematic procedures for sizing photovoltaic pumping system, using water tank storage," *Energy Policy*, vol. 37, no. 4, pp. 1489–1501, Apr. 2009.

[7] A. A. Ghoneim, "Design optimization of photovoltaic powered water pumping systems," *Energy Convers. Manag.*, vol. 47, no. 11–12, pp. 1449–1463, 2006.

[8] C. Moulay-Idriss and B. Mohamed, “Application of the DTC control in the photovoltaic pumping system,” *Energy Convers. Manag.*, vol. 65, pp. 655–662, Jan. 2013.

[9] A. Forcos and C. Marinescu, “Motor pump group efficiency in a wind energy pumped storage system,” *Adv. Top. Electr. Eng. (ATEE), 2011 7th Int. Symp.*, pp. 1–6, May 2011.

[10] R. N. Clark, “Wind-electric water pumping systems for rural domestic and livestock water,” *Proc. Eur. Wind Energy Assoc*, pp. 768–777, 1994.

[11] R. N. Clark, “Comparison of two mechanical windmill for pumping water,” in *Annual conference and exhibition of the American Wind Energy Asociation*, 1995.

[12] R. N. CLARK, *Energy, Resources and Environment*. Elsevier, 1982, pp. 520–527.

[13] F. C. Vosper and R. N. Clark, “Water Pumping with Autonomous Wind Generated Electricity,” *Trans. ASAE*, vol. 28, no. 4, pp. 1305–1308, 1985.

[14] R. N. Clark and B. Vick, “Determining the proper motor size for two wind turbines used in water pumping,” *Wind Energy 1995*, pp. 65–72, 1995.

[15] B. D. Vick, R. N. Clark, and P. O. Drawer, “Testing of a 2-kilowatt wind-electric system for water pumping,” *AWEA Wind.*, 2000.

[16] B. A. Neal and R. N. Clark, “Speed Control of a Small Wind Turbine Using Electrical Loading,” 2007.

[17] D. R. Cagle, A. D. May, B. D. Vick, and A. J. Holman, “Evaluation of Airfoils for Small Wind Turbines.”

[18] G. Manfrida and R. Secchi, “Seawater pumping as an electricity storage solution for photovoltaic energy systems,” *Energy*, vol. 69, pp. 470–484, May 2014.

[19] Mike and Pemberton, “Variable speed pumping: myths and legends,” *World Pumps*, vol. 2005, no. 460, pp. 22–24, 2005.

[20] J. Saldarriaba, *Hidraulica de Tuberias*. McGraw Hill, 1998.

Conclusions

The supply of water and energy is now a major challenge for the development of agriculture. Both water and energy are scarce resources in Chile.

Diversification of energy sources is very important to reduce electricity costs in an energy mix dominated by fossil fuels and conventional hydropower.

When drought events occur, electricity prices increase and result in increased production costs. This is especially important for small farmers in the country, whose main operating cost is electricity.

The configurations of pumping water with wind power, as described in this thesis, are a direct contribution to the reduction of production costs of small farmers, and these also represent another energy alternative.

Wind power systems with batteries are often used in pumping water. However, the evaluation of a wind-electric pumping system indicates that power losses in the electrical components, rectifier, batteries and inverter are approximately 51% of the electrical power generated. Most power loss occurs in the batteries, representing an average of 22%, while losses in the inverter and rectifier represent 14% and 5%, respectively.

Since power losses during the conversion process are considerable, especially in the battery bank, this study developed a direct coupled wind-electric pumping system with a power converter, in which water is stored in a tank. This system worked at variable rotational speed through a control strategy of the power converter, which allowed controlling the output voltage frequency. The minimum rotational speed in which the system pumped water reached

a minimum value of 50% of the rated speed for a working pressure of 10 m. It was observed that the higher the pumping pressure, the higher the rotational speed.

The control strategy with variable V/f ratio MPPT allowed increasing all the power generated by the PMG, approaching the maximum power curve for working pressures higher than 25 m. The power required by the pump could be increased to the limit established in the rated value of the pump current.

The efficiency of the power converter fluctuated between 70% and 95% depending on the load condition; overall energy losses were about 33.5%, including losses in the rectifier.

When working at a variable rotational speed, the peripheral pump showed a wider range of rotational speed interval than the centrifugal pump. Furthermore, by adding the effect of the MPPT strategy of variable V/f ratio, the rotational speed of the pump increased and higher pumping flows were obtained, especially for pressures between 20 and 30 m, compared to the linear V/f ratio. The maximum increase in flow was 15%, whereas an 8% increase was recorded when working in extreme zones of the pressure curve.

The power capacity of the system can meet water needs for small traditional agriculture, based on a single-family unit. Therefore, this pumping system could supply an important part of the electricity demand, and consequently reduce operating costs.

The direct drive wind-electric pumping system with power converter developed in this thesis can pump water without the use of a battery bank and with gravitational energy storage. This constitutes a great advantage if we consider that batteries have a high cost, a shorter useful life and efficiency when compared to the rest of the system components. In addition, the pumping system uses traditional pumps so that these can be easily replaced in case of failure.

Finally, wind pumping systems are an alternative that should be included in agriculture.

Future Research

The efficiency of wind-electric pumping systems directly affects the relationship between the cost and the useful power of these systems. The technologies for electrical power storage available at present have a negative impact on the cost of systems. This represents a problem that has not been solved in this area. Moreover, power converters have achieved a high degree of maturity, existing topologies capable of generating nearly undistorted sinusoidal voltage. Such converters require complex control strategies with high processing capacity, without increasing costs significantly. However, data processing capacity, memory and speed of microcontrollers have increased in the last decade, and this has made their implementation possible. The use of these technologies would reduce power losses in the system and generate the harmonic content, which in turn would reduce the size of components to generate usable power. In order to do so, this research will study suitable control strategies for power converters used with wind-electric pumping systems.

One of the challenges to implement the power converter was to find the suitable components for the level of voltage of the permanent magnet generator. This led to the use of one-phase electropumps rather than three-phase ones because the former require a lower maximum operating voltage. An increase in the voltage of the system would allow using three-phase systems, with the possibility of increasing the power level of the application and the pumping capacity. This increased power in direct drive pumping systems will be addressed by developing control algorithms especially designed for three-phase systems, which require the control of a larger number of transistors.

Finally, in order to replicate the system and expand its use, it is necessary to know the potential of the wind resource at the national level, particularly in areas where agricultural activities take place; wind speed and direction are largely influenced by geographical features. Therefore, prospecting projects will be developed in locations of interest.

List of References

[1] "Censo 2012." [Online]. Available: http://www.censo.cl. [Accessed: 10-Mar-2014].

[2] "Censo agropecuario 2007," 2007. [Online]. Available: http://www.censoacropecuario.cl. [Accessed: 20-Mar-2013].

[3] U. de C. Departamento de Geofísica, *Proyecto Eolo Evaluación del Potencial Eólico Nacional*, Informe Final. Santiago, 1993.

[4] O. Ozgener, "A small wind turbine system (SWTS) application and its performance analysis," *Energy Convers. Manag.*, vol. 47, no. 11–12, pp. 1326–1337, 2006.

[5] J. Saldarriaba, *Hidraulica de Tuberias*. McGraw Hill, 1998.

[6] R. N. Clark, "Wind-electric water pumping systems for rural domestic and livestock water," *Proc. Eur. Wind Energy Assoc*, pp. 768–777, 1994.

[7] R. N. Clark and B. Vick, "Determining the proper motor size for two wind turbines used in water pumping," *Wind Energy 1995*, pp. 65–72, 1995.

[8] E. Muljadi, G. Nix, and J. T. Bialasiewicz, "Analysis of the dynamics of a wind-turbine water-pumping system," in *Power Engineering Society Summer Meeting, 2000. IEEE*, 2000, vol. 4, pp. 2506 –2519 vol. 4.

[9] M. Velasco, O. Probst, and S. Acevedo, "Theory of wind-electric water pumping," *Renew. Energy*, vol. 29, no. 6, pp. 873–893, 2004.

[10] R. D. Fernandez, R. J. Mantz, and P. E. Battatotto, "Sliding Mode Control for Efficiency Optimization of Wind Electrical Pumping Systems," *Wind Energy*, vol. 6, no. 2, pp. 161–178, 2003.

[11] B. D. Vick, R. N. Clark, and P. O. Drawer, "Testing of a 2-kilowatt wind-electric system for water pumping," *AWEA Wind.*, 2000.

[12] M. S. Miranda, R. O. C. Lyra, and S. R. Silva, "An alternative isolated wind electric pumping system using induction machines," *Energy Conversion, IEEE Trans.*, vol. 14, no. 4, pp. 1611–1616, 1999.

[13] M. Velasco, O. Probst, and S. Acevedo, "Theory of wind-electric water pumping," *Renew. Energy*, vol. 29, no. 6, pp. 873–893, May 2004.

[14] A. J. Bowen, N. Zakay, and R. L. Ives, "The field performance of a remote 10 kW wind turbine," *Renew. Energy*, vol. 28, no. 1, pp. 13–33, 2003.

[15] K. Tan and S. Islam, "Optimum control strategies in energy conversion of PMSG wind turbine system without mechanical sensors," *Energy Conversion, IEEE Trans.*, vol. 19, no. 2, pp. 392–399, 2004.

[16] M. Ermis, H. B. Ertan, E. Akpinar, and F. Ulgut, "Autonomous wind energy conversion system with a simple controller for maximum-power transfer," vol. 139, no. 5. pp. 421–428, 1992.

[17] R. . Bansal, T. . Bhatti, and D. . Kothari, “On some of the design aspects of wind energy conversion systems,” *Energy Convers. Manag.*, vol. 43, no. 16, pp. 2175–2187, Nov. 2002.

[18] A. M. De Broe, S. Drouilhet, and V. Gevorgian, “A peak power tracker for small wind turbines in battery charging applications,” *Energy Conversion, IEEE Trans.*, vol. 14, no. 4, pp. 1630–1635, 1999.

[19] H. Daniel, *Electronica de Potencia*, 2da ed. Madrid: Prentice Hall, 2001.

[20] C. Armenta-Deu, “Prediction of battery behaviour in SAPV applications,” *Renew. Energy*, vol. 28, no. 11, pp. 1671–1684, Sep. 2003.

[21] CNE-PNUD-GEF, “Chilean Official Standard NCh 2946, Wind turbine generator systems.,” Santiago, Chile, 2005.

[22] “Xantrex Technologiy Inc. Installation and operator’s manual for the Xantrex DR Series Inverter/Charger. Arlington, USA.,” 2000. [Online]. Available: http://www.xantrex.com.

[23] IEEE, “IEEE Recommended Practice for Sizing Lead-Acid Batteries for Stand-Alone Photovoltaic (PV) Systems.” 2010.

[24] D. D. Lara, G. G. Merino, B. J. Pavez, and J. A. Tapia, “Efficiency assessment of a wind pumping system,” *Energy Convers. Manag.*, vol. 52, no. 2, pp. 795–803, 2011.

[25] T. Ouchbel, S. Zouggar, M. L. Elhafyani, M. Seddik, M. Oukili, a. Aziz, and F. Z. Kadda, “Power maximization of an asynchronous wind turbine with a variable speed feeding a centrifugal pump,” *Energy Convers. Manag.*, vol. 78, pp. 976–984, Feb. 2014.

[26] J. S. Anagnostopoulos and D. E. Papantonis, “Pumping station design for a pumped-storage wind-hydro power plant,” *Energy Convers. Manag.*, vol. 48, no. 11, pp. 3009–3017, Nov. 2007.

[27] B. D. Vick and R. N. Clark, “Performance of wind-electric and solar-PV water pumping systems for watering livestock,” *Trans. Soc. Mech. Eng. J. Sol. ENERGY Eng.*, vol. 118, pp. 212–216, 1996.

[28] D. Fiaschi, R. Graniglia, and G. Manfrida, “Improving the effectiveness of solar pumping systems by using modular centrifugal pumps with variable rotational speed,” *Sol. Energy*, vol. 79, no. 3, pp. 234–244, 2005.

[29] A.-K. Daud and M. M. Mahmoud, “Solar powered induction motor-driven water pump operating on a desert well, simulation and field tests,” *Renew. Energy*, vol. 30, no. 5, pp. 701–714, 2005.

[30] I. Schiemenz and M. Stiebler, “Control of a permanent magnet synchronous generator used in a variable speed wind energy system,” in *Electric Machines and Drives Conference, 2001. IEMDC 2001. IEEE International*, 2001, pp. 872–877.

[31] A. B. Raju, K. Chatterjee, and B. G. Fernandes, “A simple maximum power point tracker for grid connected variable speed wind energy conversion system with reduced

switch count power converters," in *Power Electronics Specialist Conference, 2003. PESC '03. 2003 IEEE 34th Annual*, 2003, vol. 2, pp. 748 – 753 vol.2.

[32] E. Koutroulis and K. Kalaitzakis, "Design of a maximum power tracking system for wind-energy-conversion applications," *Ind. Electron. IEEE Trans.*, vol. 53, no. 2, pp. 486–494, 2006.

[33] W.-M. Lin and C.-M. Hong, "Intelligent approach to maximum power point tracking control strategy for variable-speed wind turbine generation system," *Energy*, vol. 35, no. 6, pp. 2440–2447, Jun. 2010.

[34] D. Bang, H. Polinder, G. Shrestha, and J. A. Ferreira, "Review of generator systems for direct-drive wind turbines," in *European Wind Energy Conference & Exhibition, Belgium*, 2008, pp. 1–11.

[35] G. Inc., "PMG1600." [Online]. Available: www.ginglong.com.

[36] T. Ouchbel, S. Zouggar, M. L. Elhafyani, M. Seddik, M. Oukili, A. Aziz, and F. Z. Kadda, "Power maximization of an asynchronous wind turbine with a variable speed feeding a centrifugal pump," *Energy Convers. Manag.*, vol. 78, pp. 976–984, Feb. 2014.

[37] E. R. Collins, "Torque and slip behavior of single-phase induction motors driven from variable frequency supplies," in *Conference Record of the 1990 IEEE Industry Applications Society Annual Meeting*, 1990, pp. 61–66.

[38] D. Yildirim and M. Bilgic, “PWM AC chopper control of single-phase induction motor for variable-speed fan application,” *Industrial Electronics, 2008. IECON 2008. 34th Annual Conference of IEEE*. pp. 1337–1342, 2008.

[39] A. Z. Latt and N. N. Win, “Variable Speed Drive of Single Phase Induction Motor Using Frequency Control Method,” *Education Technology and Computer, 2009. ICETC ’09. International Conference on*. pp. 30–34, 2009.

[40] S. B. Kjaer, J. K. Pedersen, and F. Blaabjerg, “A Review of Single-Phase Grid-Connected Inverters for Photovoltaic Modules,” *IEEE Trans. Ind. Appl.*, vol. 41, no. 5, pp. 1292–1306, Sep. 2005.

[41] L. Clotea, A. Forcos, C. Marinescu, and M. Georgescu, “Power losses analysis of two-level and three-level neutral clamped inverters for a wind pump storage system,” *Optim. Electr. Electron. Equip. (OPTIM), 2010 12th Int. Conf.*, pp. 1174–1179, May 2010.

[42] B. Ismail, S. Taib, A. R. M. Saad, M. Isa, and C. M. Hadzer, “Development of a Single Phase SPWM Microcontroller-Based Inverter,” in *2006 IEEE International Power and Energy Conference*, 2006, pp. 437–440.

[43] A. A. Qazalbash, A. Amin, A. Manan, and M. Khalid, “Design and implementation of microcontroller based PWM technique for sine wave inverter,” in *2009 International Conference on Power Engineering, Energy and Electrical Drives*, 2009, pp. 163–167.

[44] R. Kot, M. Rolak, and M. Malinowski, “Comparison of maximum peak power tracking algorithms for a small wind turbine,” *Math. Comput. Simul.*, vol. 91, pp. 29–40, May 2013.

[45] Feel-Soon Kang, Sung-Jun Park, Han-Woong Park, and Cheul-U Kim, “A novel high performance single-phase 3-level PWM inverter,” in *ISIE 2001. 2001 IEEE International Symposium on Industrial Electronics Proceedings (Cat. No.01TH8570)*, 2001, vol. 2, pp. 922–927.

[46] G. G. Merino, L. O. Lagos, and J. E. Gontupil, “Monitoring and evaluation of a direct coupled photovoltaic pumping system,” *Appl. Eng. Agric.*, vol. 24, no. 3, pp. 277–284, 2008.

[47] D. D. Lara, G. G. Merino, B. J. Pavez, and J. a. Tapia, “Efficiency assessment of a wind pumping system,” *Energy Convers. Manag.*, vol. 52, no. 2, pp. 795–803, Feb. 2011.

[48] K. MEAH, S. ULA, and S. BARRETT, “Solar photovoltaic water pumping—opportunities and challenges,” *Renew. Sustain. Energy Rev.*, vol. 12, no. 4, pp. 1162–1175, May 2008.

[49] E. Larralde and R. Ocampo, “Pump selection: a real example,” *World Pumps*, vol. 2010, no. 3, pp. 28–33, 2010.

[50] A. Hamidat and B. Benyoucef, “Systematic procedures for sizing photovoltaic pumping system, using water tank storage,” *Energy Policy*, vol. 37, no. 4, pp. 1489–1501, Apr. 2009.

[51] A. A. Ghoneim, “Design optimization of photovoltaic powered water pumping systems,” *Energy Convers. Manag.*, vol. 47, no. 11–12, pp. 1449–1463, 2006.

[52] C. Moulay-Idriss and B. Mohamed, “Application of the DTC control in the photovoltaic pumping system,” *Energy Convers. Manag.*, vol. 65, pp. 655–662, Jan. 2013.

[53] A. Forcos and C. Marinescu, “Motor pump group efficiency in a wind energy pumped storage system,” *Adv. Top. Electr. Eng. (ATEE), 2011 7th Int. Symp.*, pp. 1–6, May 2011.

[54] R. N. Clark, “Comparison of two mechanical windmill for pumping water,” in *Annual conference and exhibition of the American Wind Energy Asociation*, 1995.

[55] R. N. CLARK, *Energy, Resources and Environment*. Elsevier, 1982, pp. 520–527.

[56] F. C. Vosper and R. N. Clark, “Water Pumping with Autonomous Wind Generated Electricity,” *Trans. ASAE*, vol. 28, no. 4, pp. 1305–1308, 1985.

[57] B. A. Neal and R. N. Clark, “Speed Control of a Small Wind Turbine Using Electrical Loading,” 2007.

[58] D. Cagle, A. Mays, B. Vick, and A. Holman, “Evaluation of airfoils for small wind turbines,” *Windpower*, 2006.

[59] G. Manfrida and R. Secchi, “Seawater pumping as an electricity storage solution for photovoltaic energy systems,” *Energy*, vol. 69, pp. 470–484, May 2014.

[60] Mike and Pemberton, “Variable speed pumping: myths and legends,” *World Pumps*, vol. 2005, no. 460, pp. 22–24, 2005.